

Sushan Khadka

Evaluation of Radio Anechoic Chamber

Helsinki Metropolia University of Applied Sciences

Bachelor of Engineering

Degree Programme in Electronics

Bachelor's Thesis

27 April 2017

Author(s) Title	Sushan Khadka Evaluation of Radio Anechoic Chamber
Number of Pages Date	44 pages + 3 appendices 27 April 2017
Degree	Bachelor of Engineering
Degree Programme	Electronics
Specialisation option	
Instructor(s)	Matti Fischer, Principal Lecturer
<p>The main goal of this project was to evaluate the radio anechoic chamber located on 6th floor of the electronics department building of Helsinki Metropolia University of Applied Sciences at Albertinkartu 40-42, 00150 Helsinki. From the results obtained, the performance of the anechoic chamber was determined; how well the chamber was absorbing the signals generated inside the chamber; if the antenna measurements that were being carried out inside the chamber were accurate.</p> <p>The chamber was evaluated using APC method and VSWR method which are the two most common type of techniques used for determining the reflectivity of an anechoic chamber. In each method, two identical patch antennas tuned at 735 MHz frequency were used and the measurements were recorded using the network analyzer. The final value of reflectivity calculated from both methods were compared to the commercial standard and thus the evaluation of the chamber was realized.</p> <p>From the calculated results, the reflectivity of the chamber was found to be quite supporting with the tested frequency and the performance of the pyramidal absorber. In addition, the anechoic chamber seems to be complying with the commercial standard for radiated emission test.</p> <p>The main target of the project fulfilled the requirement of the frequency that was used for the measurements. However, an anechoic chamber cannot be evaluated relying on one frequency only. The reflectivity of the chamber can be investigated at various frequencies and proper evaluation of the chamber can be achieved. The reflectivity value of the anechoic chamber calculated during this project can give an individual idea to some extent regarding the performance of the chamber and inconsistency in the measurements that is being carried out inside the chamber.</p>	
Keywords	RF Anechoic Chamber, Anechoic Chamber Reflectivity, Pyramidal Absorber, Ferrite Tiles, VSWR Method, APC Method

Contents

1	Introduction	1
2	EM Waves	2
3	Antennas	5
3.1	Types of Antennas	6
3.1.1	Dipole Antenna	6
3.1.2	Microstrip or Patch Antenna	7
3.1.3	Biconical Antenna	9
3.2	Antenna Measurements	9
3.2.1	Radiation Pattern	10
3.2.2	Gain, Directivity and efficiency measurements	13
4	Anechoic Chamber	14
4.1	RF Absorbers	16
4.1.1	Pyramidal Absorbers	20
4.1.2	Ferrite Tile Absorbers	24
5	Anechoic chamber facility at Metropolia	28
6	Reflectivity of the Anechoic Chamber	32
6.1	VSWR Method	32
6.1.1	Measurement Procedure	33
6.1.2	Measurement Results and Calculations	35
6.2	APC Method	38
6.2.1	Measurement Procedure	38
6.2.2	Measurement Results and Calculations	38
7	Conclusion	41
	References	42
	Appendices	
	Appendix 1. Transversal Scan Data	
	Appendix 2. Longitudinal Scan Data	
	Appendix 3. Transversal Scan Data at different angles of antenna	

List of Abbreviations

dB	Decibel
MHz	Megahertz
GHz	Gigahertz
EM	Electromagnetic
RF	Radio Frequency
EMC	Electromagnetic Compatibility
EMI	Electromagnetic Interference
VSWR	Voltage Standing Wave Ratio
APC	Antenna Pattern Comparison
CISPR	International Special Committee on Radio Interference

1 Introduction

Technology is becoming more sophisticated and inevitable part of the modern world. Various new inventions and innovations have been made over the past few decades. Every big electrical and electronic company are always in search of a new idea so that they could attract customers to their products. If a company successfully manufactures an electronic equipment, they could not just launch it in the market. Since every electronic device radiates certain amount of EM (Electromagnetic) fields, they must pass the EMC (Electromagnetic Compatibility) tests. EMC test is what defines an electronic device eligible to be sold on the market, whether it is functioning as desired and if it is emitting EM waves as mentioned in EMC standards.

Every year, Metropolia offers different courses related to EMC and EMI (Electromagnetic Interference) measurements. Students must complete many laboratory exercises regarding the study of RF (Radio Frequency) emission of various electronic devices and its impact on other electronic equipment. As a part of laboratory exercise, students are also supposed to study the behaviour of different types of antennas. Besides, many students write their bachelor thesis based on RF related fields. It is very much essential for them to know the behaviour of the equipment they have designed.

It is very hard to study the characteristics of an equipment in an open environment as there are lot of noises present in the environment. Each electronic device present in the test site can interfere with the measurements being taken. Therefore, an anechoic chamber is what comes in use at these conditions as it provides reflection free zone where no signals can enter from the outside world and absorbs all signals generated inside the chamber.

The sole purpose of this thesis project was to evaluate the anechoic chamber facility provided by Metropolia located at the 6th floor of electronics department building at Albertinkartu. The project was mainly focused on reflectivity level measurement of the anechoic chamber using the available antennas and a network analyzer in the campus. The evaluation of the chamber was achieved as a function of location and as a function of frequency. Thus, based on the obtained measurements, the anechoic chamber was determined if it was suitable for accurate measurements (maybe even commercially).

2 EM Waves

Whenever there is transmission or receiving of signals in space by an antenna, there exists radio waves. Radio waves are EM waves and are often called EM radiations. In 1865, James Clerk Maxwell (1831-1879) published a paper 'A dynamical Theory of the Electromagnetic Field' which demonstrated that EM waves are vibrations of both electric and magnetic fields perpendicular to each other and travel with the speed of light.

The wave equation of electric field E_x oscillating in x-axis direction and travelling in z-axis direction and magnetic field H_y oscillating in y direction and travelling in z-direction as shown in the Figure 1 can be represented as [1]:

$$E_x(z, t) = E_0 \sin(\omega t - kz + \phi) \quad (1)$$

$$H_y(z, t) = H_0 \sin(\omega t - kz + \phi) \quad (2)$$

where:

k = Wave number

ω = Angular frequency [radians/second]

T = Time period for wave to complete one cycle [seconds]

f = Frequency of the oscillating wave in cycles per second [Hertz]

t = Any instant of time

z = Value of z – axis coordinate at time t

ϕ = Phase angle of the waves; at $z = 0$ and $t = 0$

The conclusion of Maxwell's equation relates electric field and magnetic field as:

$$H_y(z, t) = \frac{1}{c} E_x(z, t)$$

$$H_0 \sin(\omega t - kz + \phi) = \frac{1}{c} E_0 \sin(\omega t - kz + \phi) \quad (3)$$

Hence, at any points, the ratio of magnitude of electric field to the magnetic field as shown in equation (4) gives the speed of light or EM wave in space denoted by 'c'.

$$c = \frac{|E|}{|H|} \quad (4)$$

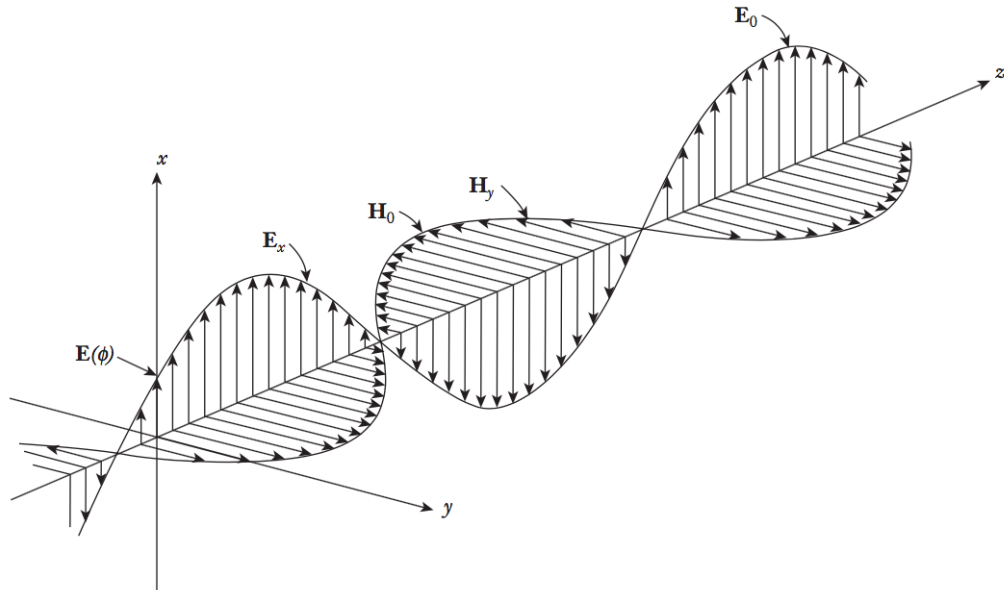


Figure 1. Electromagnetic wave in free space [1]

The components of electric field and magnetic field are in phase in space and time as shown in the Figure 1. This means that the minimum and the maximum value for the electric and magnetic field occurs for the same values of time t and fixed value of z (points at waves oscillating direction). [1]

Frequency or wavelength of the EM radiations could be determined knowing either of the terms in free space. Since the speed of light is the speed of radio wave, the relation between velocity, frequency and wavelength of the EM or radio wave is given by:

$$v_0 = \lambda \cdot f \quad (5)$$

Where:

$v_0 = c = 3 \times 10^8 \text{ m/s} = \text{Velocity of radio wave in vacuum}$

$\lambda = \text{Wavelength of EM wave [metre]}$

$f = \text{Frequency of the EM wave [Hertz]}$

The propagating nature of EM radiations are much like water waves. The velocity, amplitude and direction of the radio waves vary and are absorbed when it propagates through different medium. For example, the propagative nature of radio wave changes when it passes through concrete walls and trees. Similarly, taller buildings can reflect

radio waves scattering it into various directions. In addition, radio waves with certain higher frequencies ($f \geq 10$ GHz) are absorbed largely by bigger rain droplets.

When EM wave is radiated from its source, it spreads out in all directions as if it is covering the surface of the sphere [2]. More the wave travels, more the distance between the source and the radiation is increased thus, increasing the area of the sphere. In other words, the power density (P_D) at any point in space is inversely proportion to the distance between the source and at that point. Mathematically,

$$P_D \propto \frac{1}{R_D^2} \quad (6)$$

Where:

$R_D =$ Radius of the sphere

Equation (7) is also called the inverse square law. Hence, the power density at any point can be calculated by knowing the transmitted power from the source as shown in the equation (7) below:

$$P_D = \frac{P_t}{4\pi R_D^2} \quad (7)$$

Where:

$P_t =$ Total power radiated from the source

The signal levels of free space EM wave are very low, that is, in the order of -100 dBm (3 μ V). Since there are lot of other energies present in the environment, the signal can be easily masked off by these energies. Consequently, it becomes very difficult to characterize an electrical equipment based on EMC in an open environment. Shielding enclosures could be a choice that provides an isolation performance of about 100 dBs. But EM waves are reflected back and forth around all the corners of the shielded enclosure due to which a complex wavefront is formed at the test antenna region preventing the formation of uniform plane wave. So, a closed site what we call an anechoic chamber that is free from all sorts of wave interferences and reflections is required to evaluate an electronic device. [3]

3 Antennas

Webster's Dictionary defines an antenna as "a usually metallic device (as a rod or wire) for radiating or receiving radio waves." *The IEEE Standard Definitions of Terms for Antennas (IEEE Std 145–2013)* defines an antenna as "a part of the system designed for radiating and receiving EM waves." In other words, an antenna acts a transitional system between transmitting line (guiding device) and free space which can be seen in the Figure 2. The transmitting line can be any form such as a coaxial cable or a waveguide that can be used for transporting radio waves from an antenna to the receiver, or from a transmitter to an antenna. [4]

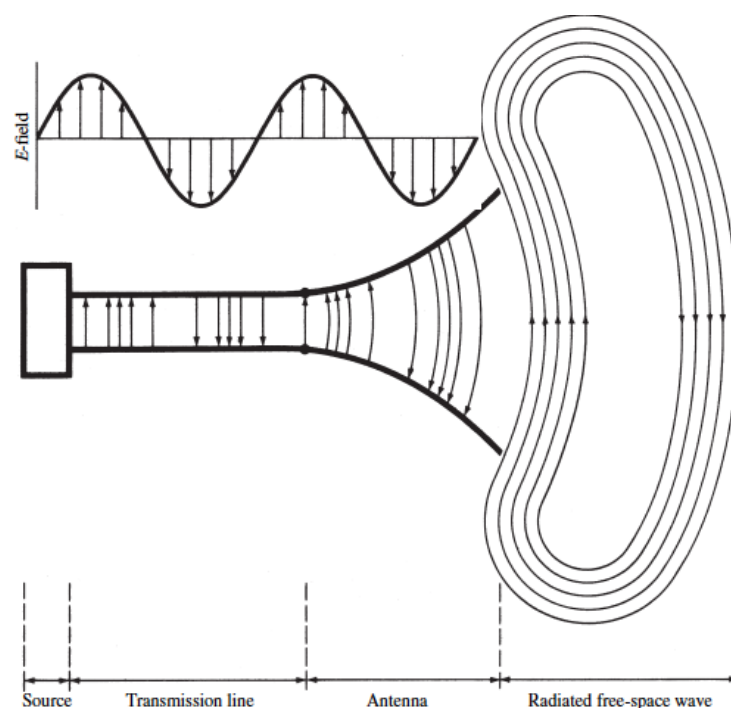


Figure 2. An antenna represented as a transitional device [4]

In modern wireless system, antennas are not only used for transmitting and receiving radio energy, but also for optimizing or emphasizing the radio energy in desired directions and suppressing it in others. Hence, antennas also act as a directional device. They can be used in different form as required by the system; an antenna can be a piece of electric wire, a lens, a reflector, an array and so on. [4]

Antennas are key element to bring revolution in the communication system. Over the past 60 decades, antenna technology developed so much that most of the major advancements that happened during this era are in daily use today. Almost all the electronic

equipment that has wireless communication system contain or require an antenna as a main component. A good example can be a television or a radio whose broadcasting performance can be improved by installing a suitable antenna. An antenna is required to a communication system for the same purpose that eyes and eyeglasses are required to a human. [4]

3.1 Types of Antennas

There were three different types of antennas available to measure in this project. The antennas were pair of dipole antennas, a pair of microstrip patch antennas and an EMC biconical antenna. Two of the dipole antennas and microstrip patch antennas were developed by the past students, whereas the biconical antenna was a company manufactured antenna.

3.1.1 Dipole Antenna

Dipole antenna is the most common type of antenna that has been widely used since the beginning days of radio. The simplicity and the efficiency that a dipole antenna provides in communications can be a reason for it to be considered as a popular and a worthy device. The construction of the dipole antenna is simple and most of the calculations involved in its design are quite straightforward. However, in-depth calculations are more complex like any other antennas. Dipole antennas are also used as an important element in different other antennas. [5;6]

The name dipole itself suggests that it is an antenna that consists of two poles (radiating element) or terminals such as conducting wires or metal rods in which RF current flows. The poles of the dipole antennas are symmetrical; both poles are equal in sizes and extends from the feed point to the opposite directions. These poles are the main part of a dipole antennas as its length can be used to determine impedance, operating frequency and many of the other properties. [6]

The electrical length of each radiating element in a typical dipole antenna is quarter wavelength $\left(\frac{\lambda}{4}\right)$ making the antenna half wavelength $\left(\frac{\lambda}{2}\right)$ long [6]. This is done for resonant condition and the resonance occurs when there is presence of only resistance in the impedance but no reactance at the given frequency [5].

Figure 3(a) and Figure 3(b) shows the basic structure of dipole antenna and typical half wavelength antenna respectively.

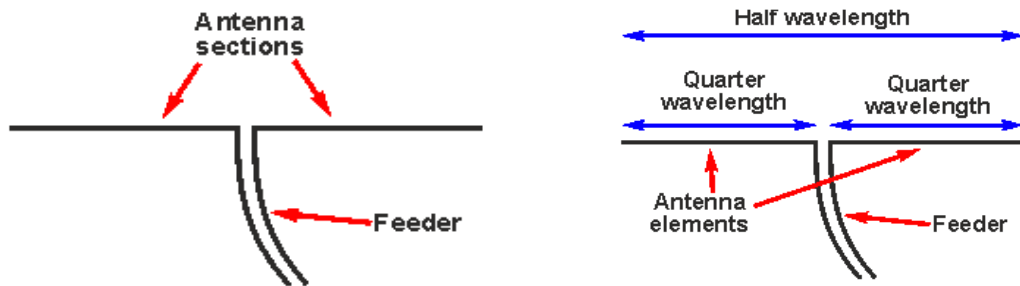


Figure 3(a). Basic structure of dipole antenna, Figure 3(b). Half wavelength dipole antenna [6]

The length of a half wave dipole antenna can be calculated by using the simple mathematical formula as shown in equations (8) and (9) below.

$$\text{Length(in metres)} = 150 \times \frac{A}{\text{frequency}} [\text{MHz}] \quad (8)$$

$$\text{Length(in inches)} = 5905 \times \frac{A}{\text{frequency}} [\text{MHz}] \quad (9)$$

Where:

A = Multiplication factor

The multiplication factor 'A' mainly depends upon the ratio of the antenna's length to the thickness of the radiating element and is generally between 0.96 and 0.98 [7]. The electrical length of the radiating element can vary from the actual length of the EM wave in free space because the wave is affected by various factors of the radiating element. In free space, the radiating elements are little bit shorter than the EM wave length [6].

3.1.2 Microstrip or Patch Antenna

Microstrip antennas are mainly used for microwave frequency. They are becoming more popular these days as they can be directly implemented in PCBs (Printed Circuit Board). At present, they are widely used in mobile phones and any other portable wireless communication devices. The basic structure of microstrip antenna consists of patch (conductive metallic strip) as radiating element and a ground plane that are separated by a dielectric substrate as shown in the Figure 4.

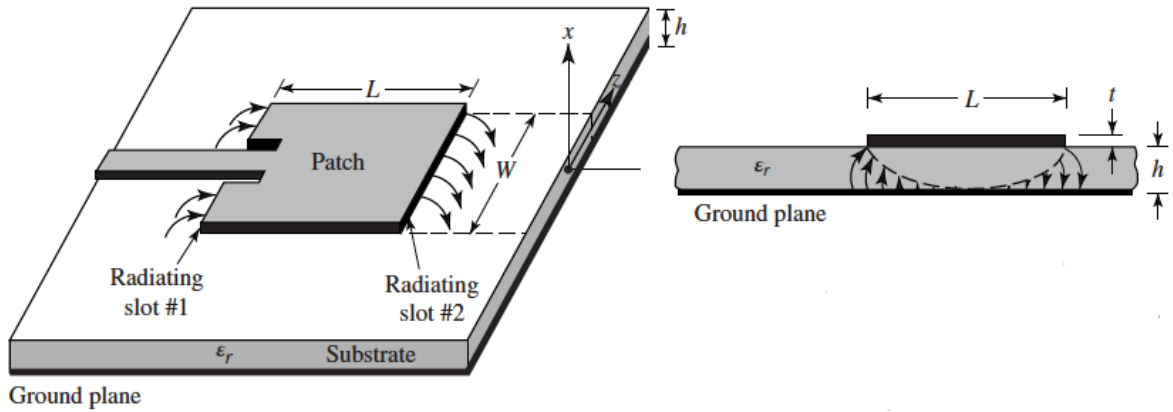


Figure 4. Basic structure of microstrip antenna [4]

The thickness t of the metallic strip and the height ' h ' (usually $0.003\lambda_0 \leq h \leq 0.05\lambda_0$) of the substrate in a microstrip antenna is very much smaller than the free space wavelength (λ_0). Similarly, the length ' L ' of a patch (radiating element) in a rectangular patch antenna is usually between $\frac{\lambda_0}{3}$ and $\frac{\lambda_0}{2}$. The design of a patch can be also triangular, square, elliptical etc. The patch of the microstrip antenna is designed so that maximum of the pattern is normal to the patch. This can be achieved by choosing suitable field configuration below the patch. [4]

The resonant frequency (f_r) of the patch antenna is a function of the length ' L ' of the radiating element. Therefore, the resonant frequency at which the patch antenna is tuned can be obtained by using the equation (10) as represented below.

$$f_r = \frac{c}{2L\sqrt{\epsilon_r}} \quad (10)$$

Different kinds of substrates can be used for designing patch antennas. The dielectric constant of these substrates is generally in the range of $2.2 \leq \epsilon_r \leq 12$. For the better performance of the antennas regarding wide bandwidth, efficiency and loosely bound EM fields, the substrates are made thicker with dielectric constants as low as possible. But this results in the bigger radiating element size that increases the expenses. On the contrary, thin substrates are used in microwave circuits as it provides tightly bound EM fields that helps to reduce unwanted coupling and radiation, and hence, results in the smaller radiating element. [4]

3.1.3 Biconical Antenna

Biconical antenna is a broadband antenna that has dipole like characteristics made by placing two cones of infinite length together [4]. It can be used for EMC testing frequency ranging from 30-300 MHz [8]. Figure 5 shows the basic structure of biconical antenna.

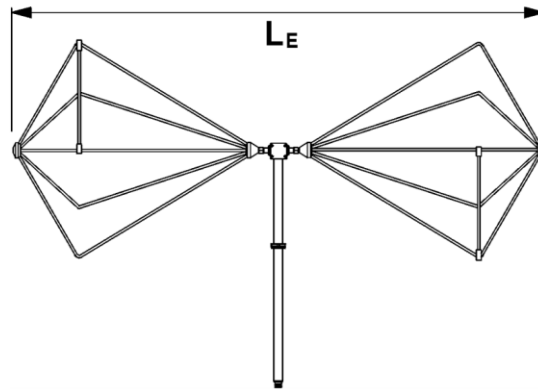


Figure 5. Biconical antenna [8]

As a broadband antenna, Biconical antenna provides a larger bandwidth with impedance closer to 50 ohms. Thus, a complicated tuning network is not required to match the impedance with the transmission line. As a practical antenna, learning about the properties and behaviour of a biconical antennas helps engineers who are interested in antenna design to understand other different types of antennas. [9]

Some general purpose for using biconical antennas are as follows:

- For emission testing at the frequency range of 20-300 MHz
- For immunity testing mainly at low frequencies
- For evaluating the testing sites such as anechoic chamber

3.2 Antenna Measurements

Most of the antenna measurement techniques were developed before and during Second World War. However, many new and advanced technologies have been introduced with the rapid development of wireless telecommunications. The basic techniques for antenna measurements, such as antenna patterns, impedance, gain, polarization and

directivity were introduced in parallel with the design of new radiating elements that are required for emerging radio and radar technologies. [10]

It was soon realized that not only good theoretical background is sufficient to determine antenna characteristics but also a sophisticated device that provides sound and accurate results. Much later in the 1960s, equipment for antenna measurements became very much necessary due to growing space, aerospace and defence industries. Hence, measuring equipment specifically designed for antenna measurements were launched commercially to meet this requirement during this period. This equipment had functions like pattern recorders, antenna ranges, signal generators, antenna positioners, antenna gain standards, etc. Nowadays, measuring equipment with advanced computer system are available that can automatically control pattern measurements, calculate antenna directivity faster, converts 2D pattern to 3D pattern and so on. [10]

The main parameters of the antenna measurements are pattern measurements and impedance measurements. Pattern measurements are the main measurement technique in antenna measurements with many subcategories such as beamwidth measurement, gain, minor lobe level and characteristics of polarization. In some cases, noise and efficiency measurements are also desired. Impedance measurement refers to the measurement of input impedance of an antenna. [1]

3.2.1 Radiation Pattern

Radiation pattern or antenna pattern is one of the fundamental property of an antenna. It can be defined as a representation of the radiative properties of an antenna either graphically or as a mathematical function. Generally, far field region is chosen for determining the radiation pattern of an antenna as function of directional coordinates. Radiation intensity, flux density, field strength, polarization and directivity are the main properties of radiation. [4]

The standard coordinate system used for representing the radiation properties of an antenna is spherical coordinate system which can be seen in the Figure 6. All the radiation properties are measured on the surface of the sphere with constant radius. Since the radius is always constant, only the angular coordinates (θ, ϕ) are required for identifying the position. Thus, the representation of radiation properties of any radiator as a function

of two angular coordinates θ and ϕ for fixed radius and frequency is called the radiation pattern of an antenna. [4]

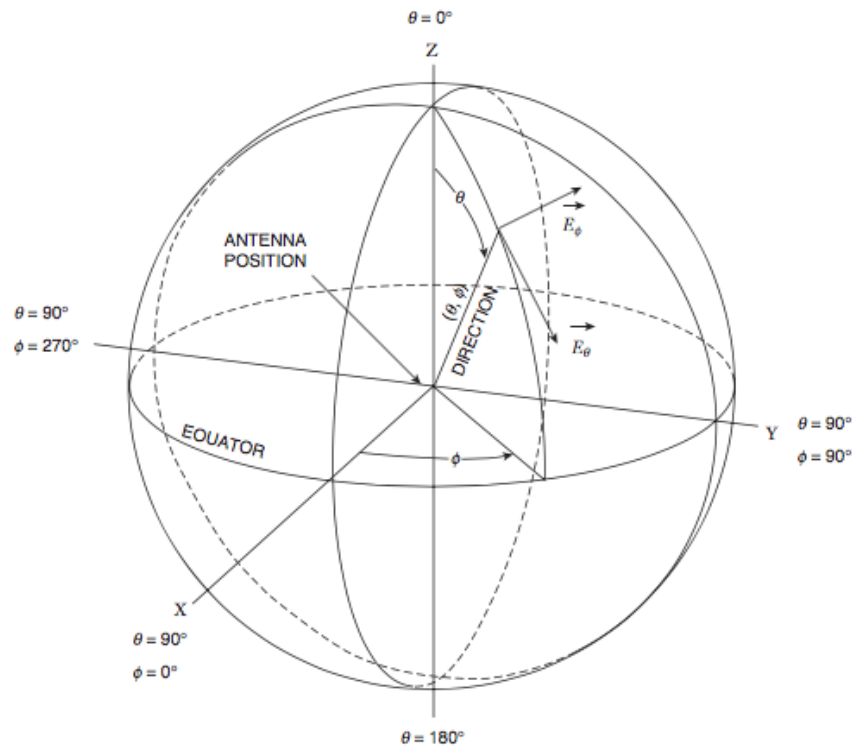


Figure 6. Geometry of spherical coordinate system [11]

An antenna radiates in all directions. Therefore, the radiation pattern of an antenna must be three dimensional. Due to impracticality, two-dimensional system is generally preferred. However, three-dimensional pattern can be constructed from the function description and with sufficient time and funds. The preferred coordinate system for two-dimensional pattern are rectangular coordinate system and polar coordinate system. These coordinate systems mainly represent the orthogonality of electric (E) and magnetic (H) field patterns. [11]

The radiation pattern of the test antenna is measured by making it as receiver antenna. The test antenna is rotated with a help of turn table at various angles at a difference of 5 degree till 360 degrees for better measurements. Once the angle reaches 360 degrees, the turn table is again rotated backward till 0 degree at a difference of 5 degrees. In case if the receiver antenna (test antenna) and the transmitting antenna (source) are reciprocal, the test antenna can be made either a transmitter or a receiver; the test antenna is made as receiver antenna in this situation. The test antenna is always kept in receiver mode unless stated. [11]

Figure 7 shows the radiation pattern of half-wavelength dipole antenna in E-plane and H-plane.

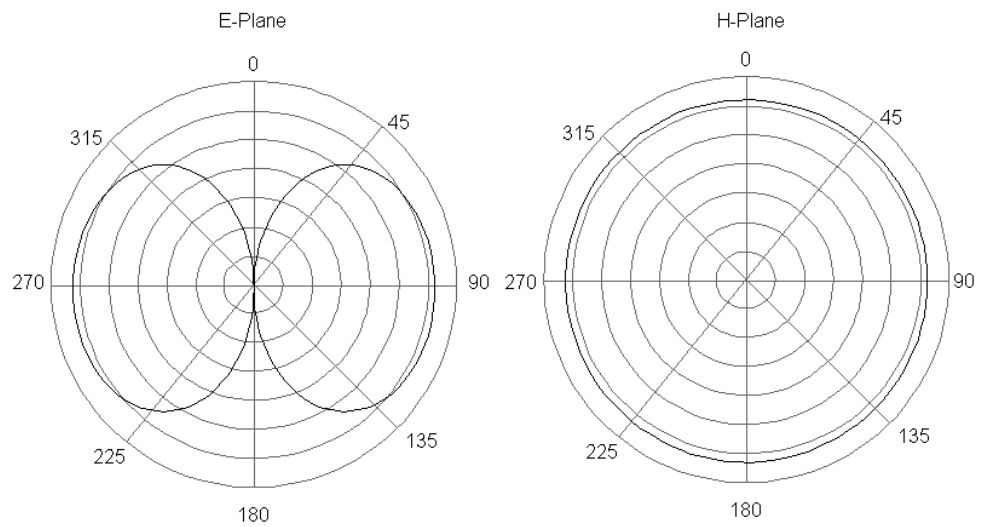


Figure 7. Radiation pattern of a dipole antenna

In the Figure 7, E-plane refers to the orientation or polarization of the radio wave and H-plane refers to the direction of maximum radiation when an antenna is vertically polarized. E-plane and H-plane are perpendicular to each other.

Similarly, Figure 8 shows the general measurement setup for antenna measurements inside the anechoic chamber with test antenna as a receiver antenna. The similar type measurement setup will be used in this project.

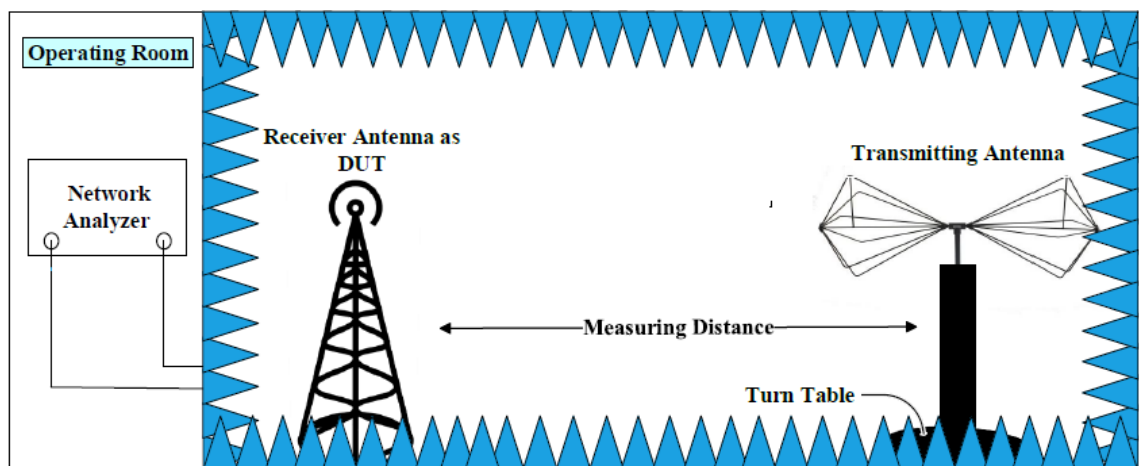


Figure 8. Measurement setup inside the anechoic chamber

3.2.2 Gain, Directivity and efficiency measurements

The IEEE Standard Definitions of Terms for Antennas (IEEE Std 145–2013) defines gain as the “The ratio of the radiation intensity in a given direction to the radiation intensity that would be produced if the power accepted by the antenna were isotropically radiated.” If R is the radius of sphere, $P_{antenna}$ is the antenna power density and P_{in} is input power of an antenna, mathematically,

$$Gain (G) = \frac{4\pi R^2 P_{antenna}}{P_{in}} \quad (11)$$

The IEEE Standard Definitions of Terms for Antennas (IEEE Std 145–2013) defines directivity as “the ratio of power radiated by the antenna in certain direction to the average power radiated by the antenna in all possible directions.” If R is the radius of sphere, $P_{antenna}$ is the antenna power density and P_{out} is output power of an antenna, mathematically,

$$Directivity (D) = \frac{4\pi R^2 P_{antenna}}{P_{out}} \quad (12)$$

From the equations (11) and (12), the relation between gain and directivity can be concluded as:

$$G = kD \quad (13)$$

Where:

$$K = \frac{P_{out}}{P_{in}} = \text{Efficiency of an antenna}$$

4 Anechoic Chamber

A simple definition of an anechoic chamber can be a room that is covered with RF absorbing materials to minimize the reflection of waves that results in the formation of standing waves.

An anechoic chamber is used for different types of antenna measurements, EMI and EMC measurements. In case of this project, it is a room that provides a platform to measure an antenna behaviour in the outside world by rotating receiver antenna through different angles. An anechoic chamber is not only a reflection free room but also a shielded room. Therefore, the destructive signals coming from the surrounding environment are blocked and the RF signals generated are absorbed by different foam absorbers and ferrite tile absorbers present inside the chamber. [12]

Figure 9 show the plain view of the rectangular anechoic chamber that uses pyramidal absorber as main RF absorbing material.

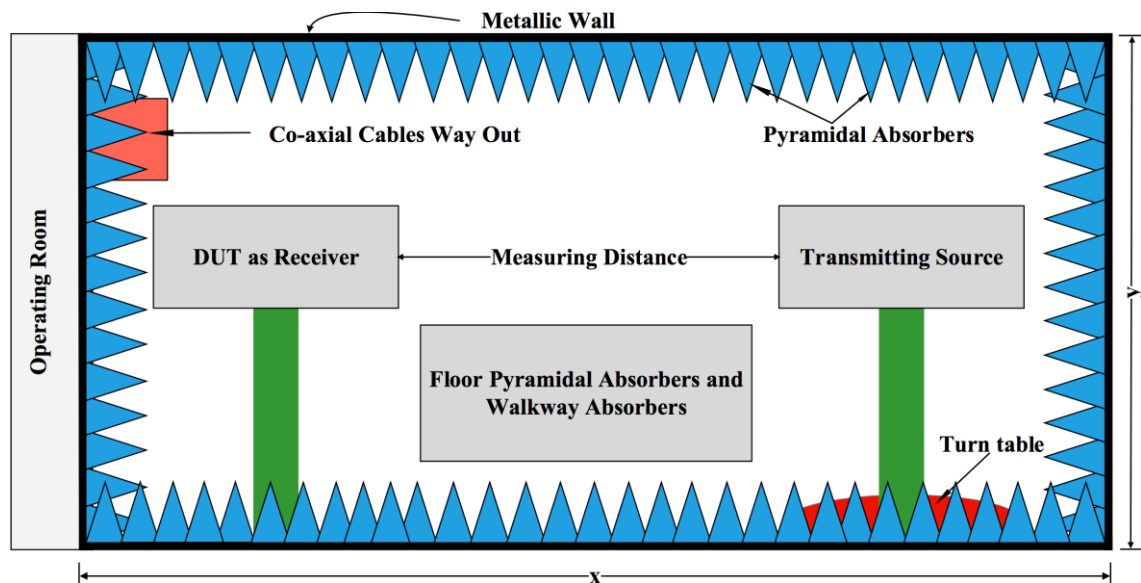


Figure 9. Typical view of an anechoic chamber with pyramidal absorber

In the Figure 9, it can be seen that the chamber is completely lined with pyramidal absorbers. There is high possibility of damaging the pyramidal absorbers with the equipment or the antennas that are going to be tested inside the chamber. So, foam absorbers or ferrite tiles are laid on the floor where receiver antenna and transmitting antenna are placed. Similarly, for antenna measurements, polarization of the antenna and distance

between the transmitter and the receiver antennas must be changed time to time. Therefore, walkway absorbers are used so that antennas can be accessed and other different types of antennas can be used whenever it is required.

To test an equipment inside the anechoic chamber, a transmitting source that emits EM signal and a device under test (DUT) as a receiver is required to receive the transmitted signal. The transmitter and receiver could be any type of antenna. The transmitted signal field strength is sampled by the receiver antenna that can be used for calculating the desired results. [13]

Within an anechoic chamber, the EMC and EMI test of electronic equipment such as radios, televisions, computers etc. and its compatibility with the standards can be evaluated with less interference from the external radiation sources like mobile phones, radios, international and local television radio stations that transmits at some point higher signal strength than the ERS (Emission Reference source). [13]

The outer surface (shell) of the anechoic chamber is metal so that it reflects signals that try to enter the chamber. Somehow if signals enter the chamber through the small holes between the wall and the door, the RF absorbers lined to the walls, ceiling and floor of the chamber helps to attenuate these signals to desired level. [13]

The working principle of an anechoic chamber is quite straightforward. Suppose an EM plane wave radiated from an antenna hits the wall of the chamber at normal incidence. This can be designed as a signal passing through a transmission line with characteristic impedance of 377 ohms as shown in the Figure 10 below. [14]

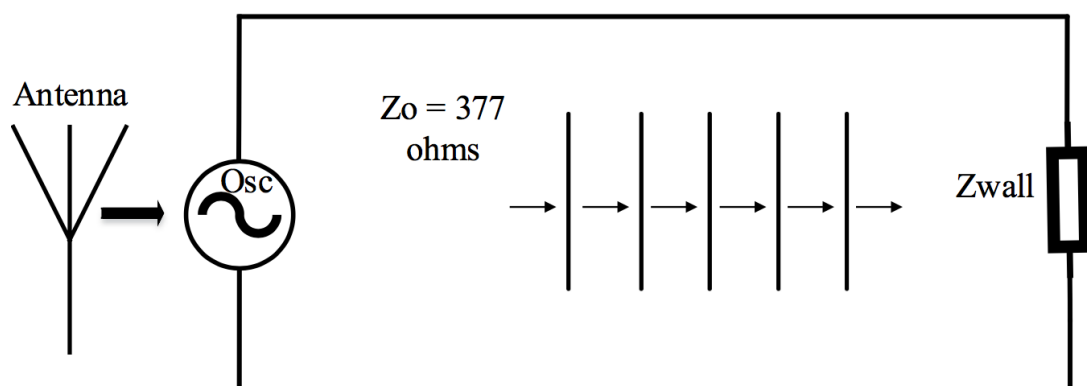


Figure 10. Anechoic chamber modelled as a transmission line circuit [14]

In the Figure 10, the antenna is modelled as a voltage source (O_{sc}) and metallic wall acts as a load (Z_{wall}). The reflectionless chamber can be created if the signal sent from the voltage source is blocked from being reflected. Since the walls of the chamber are metallic, the transmission line is short circuited at its termination. This means, all the signals are reflected as there is no dissipation of any energy in the load. Hence, the materials with absorptive property known as RF absorbers are required that absorb so much of these energies preventing the signal from being reflected. [14]

The actual inside view of the anechoic chamber with horizontally polarized microstrip dipole antennas; antenna on the right side attached to the turn table where all the antenna measurements need to be done and thus, based on those measurements whose characteristics need to be determined is shown in the Figure 11 below.

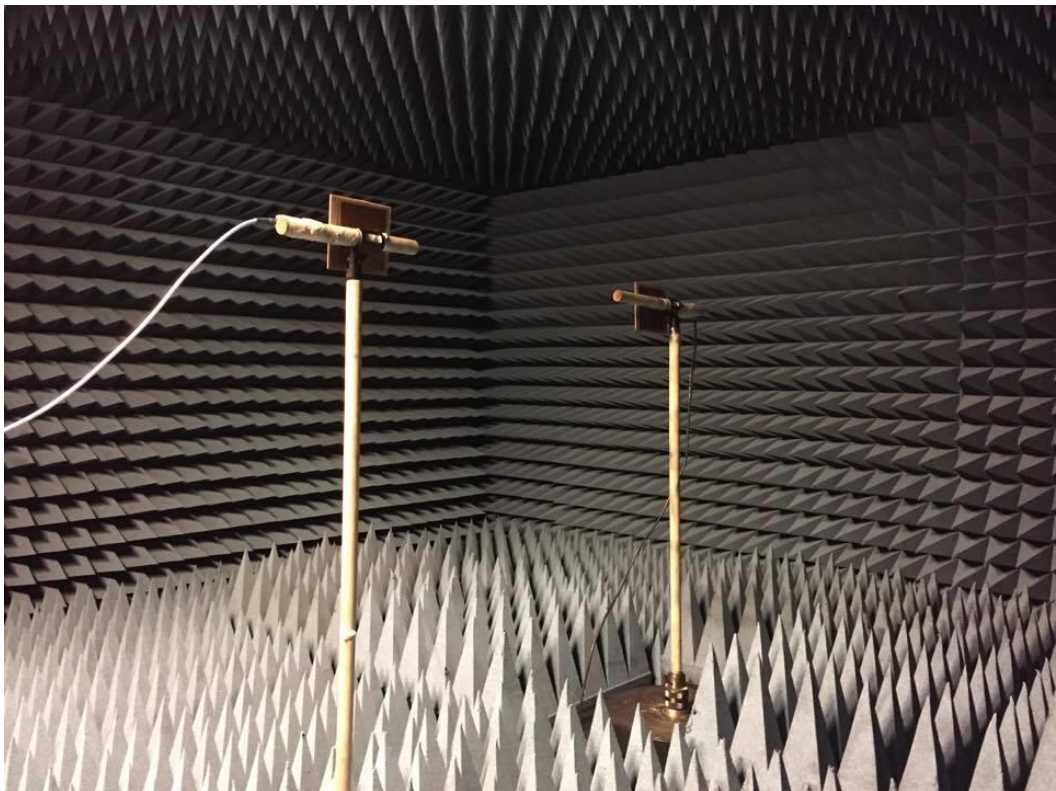


Figure 11. Inside view of the anechoic chamber

4.1 RF Absorbers

In the world of RF or microwave, absorbers are the materials that weaken the energy in an EM wave. Besides, the frequency range that an anechoic chamber operates is also determined by the type of RF absorbers that are used for lining the floor, ceiling and walls

of the chamber. The first known absorber is a quarter-wave resonant type absorber operating in the 2 GHz region which was investigated at the Naamlooze Vennotschap Machinerieen, Netherlands in 1936 [15].

There are variety of radio wave absorbers available in the market for vast range of applications to diminish undesirable radiations that could hamper operation of a system. RF absorbers can be used for both external and internal purposes. Externally, they can be used for attenuating the reflection from and transmission to certain objects. Similarly, they can be used internally for attenuating the oscillations caused by chamber resonance. In addition, they can be used for creating a free space environment (anechoic chamber) independent of all-weather condition by reducing the reflections. [16]

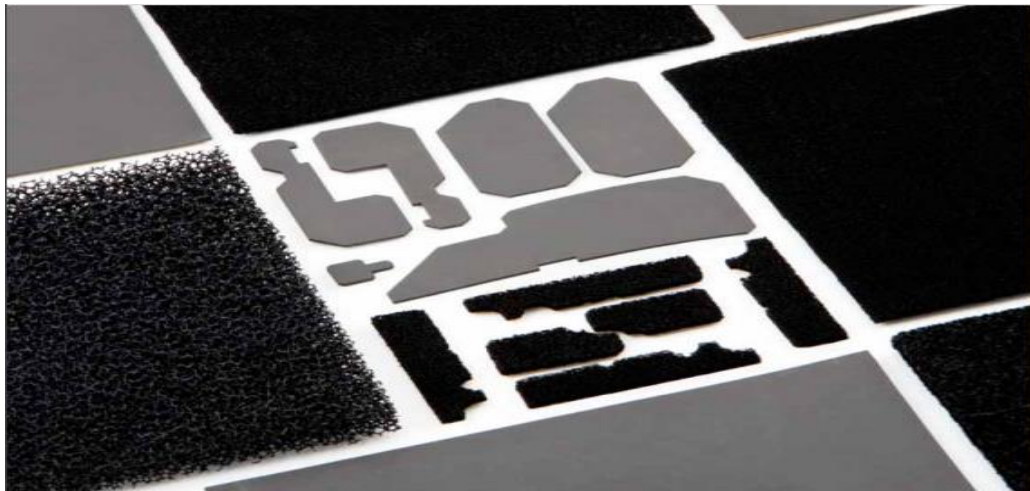


Figure 12. Different types of RF absorbing materials [17]

RF absorber are made of different materials and can be of any shape and sizes as shown in Figure 12. They can be in flexible polymer like elastomers or firm epoxy or foam or plastics. The characteristics of absorbers can be determined as per the need of test requirements. In some systems, they are used to minimize interference between circuit components [16].

The various types of RF absorbers and its characteristics in current technology are as follows:

- Polyurethane and foam absorbers
- Types: Pyramidal absorber and Wedge absorber
- High cost, larger chamber size, used for high frequency applications

- Ferrite tile absorbers
 - Types: Tiles and tile panels
 - Smaller chamber size, longer life of chamber, heavy, very expensive (cost three times more than the foam absorbers)
 - Suitable for frequency measurements (30 MHz-1 GHz)
- Polystyrene foam absorbers
 - Types: Pyramidal absorber and Wedge absorber
 - Expensive, longer life of chamber, increased chamber size than ferrite
- Hybrid absorbers
 - Types: Traditional styrene, urethane, new taper styrene, urethane
 - Maximum use of ferrite tiles above 1-60 GHz

Absorber Theory

Most of the RF or microwave absorbers contain a filler material inside a material matrix. The filler contains one or more elements which do most of the absorbing. The physical properties of an absorber can be obtained from the material matrix.

Electric permittivity and magnetic permeability determine the characteristics of an absorber. Permittivity can be defined as the measurement of resistance generated when electric field is developed inside a medium. Similarly, permeability determines an ability of a medium to assist in the development of magnetic field within itself. Mathematically, permittivity and permeability could be represented as complex which can be seen in equations (14) and (15) respectively. [16]

When an EM wave propagates through different medium, the wave is either fully transmitted or part of it is reflected or absorbed. However, amplitude of the reflected wave is the main part of interest in the anechoic chambers [12].

Figure 13 gives the basic idea how any planar EM wave generated from the source behaves inside an anechoic chamber.

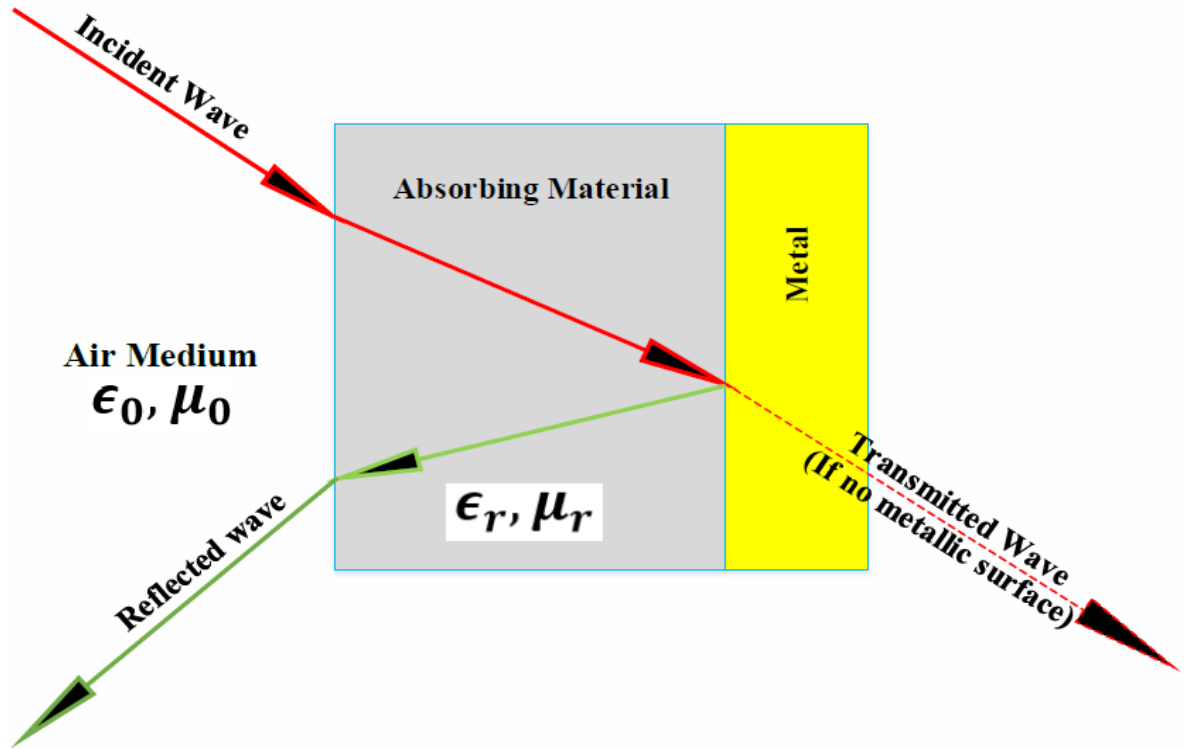


Figure 13. Basic characteristic of EM wave inside the anechoic chamber

The symbols in the Figure 13 are:

$$\epsilon_0 = 8.85 \times 10^{-12} \text{ [farad/meter] = Permittivity of air}$$

$$\mu_0 = 4\pi \times 10^{-7} \text{ [henry/meter] = Permeability of air}$$

$$\epsilon_r = \epsilon_r' - j\epsilon_r'' = \text{Permittivity of any medium (absorber in this case)} \quad (14)$$

$$\mu_r = \mu_r' - j\mu_r'' = \text{Permeability of any medium (absorber in this case)} \quad (15)$$

ϵ_r' is often called dielectric constant and varies with frequency. ϵ_r'' is the measurement of electric field loss caused by any medium [16]. Mathematically, the tangential loss in electric field could be represented as:

$$\tan \delta_E = \frac{\epsilon_r''}{\epsilon_r'} \quad (16)$$

Both components in magnetic permeability μ_r' and μ_r'' contributes for compressing the wavelength inside medium [16]. The tangential loss of magnetic field is defined as:

$$\tan \delta_M = \frac{\mu_r''}{\mu_r'} \quad (17)$$

The main concerned part in the Figure 13 is the reflected wave. Even small reflection from the absorber creates interference in receiving antenna. With reflectivity level of anechoic chamber known, error in test results can be known. Hence, the accurate results can be obtained by subtracting the reflection loss from the obtained test result. The reflection loss (RL) can be determined by calculating the following parameters.

$$Z_{in} = \sqrt{\frac{\mu_r}{\epsilon_r}} \cdot \tanh\left(j \frac{2\pi f d}{c} \cdot \sqrt{\mu_r \epsilon_r}\right) \quad (18)$$

$$\rho_l = \frac{Z_{in} - Z_0}{Z_{in} + Z_0} \quad (19)$$

$$RL = -20 \cdot \log_{10}(\rho_l) \quad (20)$$

where:

Z_{in} = Input impedance of metal backed absorbing layer [ohms]

d = Absorber thickness [meter]

f = Frequency of the radio wave [Hertz]

c = Speed of light [meter/second]

ρ_l = Reflection coefficient of metal backed absorber

$Z_0 = 377$ ohms = Characteristic impedance of air

Broadband pyramidal absorbers and ferrite tiles are extensively used in the anechoic chamber design. So, only these two types of absorbers are discussed in this document.

4.1.1 Pyramidal Absorbers

Pyramidal absorbers are dielectric absorbers and are the most common type of absorber product that are used in most of the anechoic chamber for antenna measurements and radar measurements. They are available in different shapes and sizes that provides desired impedance match between the resistive absorber medium and free space.

Pyramidal absorbers are generally made from polyurethane or polystyrene foam that is filled with conductive carbon. The absorption of RF energy from microwave frequencies from 0.5 GHz can be achieved by balancing the carbon with the shape of the foam; the foam's length can be greater than one wavelength [18]. While applying carbon to the

foam or as a secondary treatment, the carbon filled absorber should be treated with inflammable substances as per the safety standard. [12]

The carbon loaded foams are painted with different colours as the request of the customer. However, the foams are mostly painted with latex blue for good light reflectivity purpose. These paints seem not to affect the operation of the absorber for long and even modest wavelengths, but it can be disturbing at shorter wavelengths (less than an inch or so). For example, the latex blue paint degrades the reflectivity of the chamber approximately 5 dB at frequency of 95 GHz. [12]

The amount of carbon introduced in the absorbers during the production process can hugely vary the reflectivity level of the absorbers. These variations can be seen in the Figure 14 below that illustrates change in reflectivity on loading carbon with various thickness in the foam absorber corresponding to the test frequency. [12]

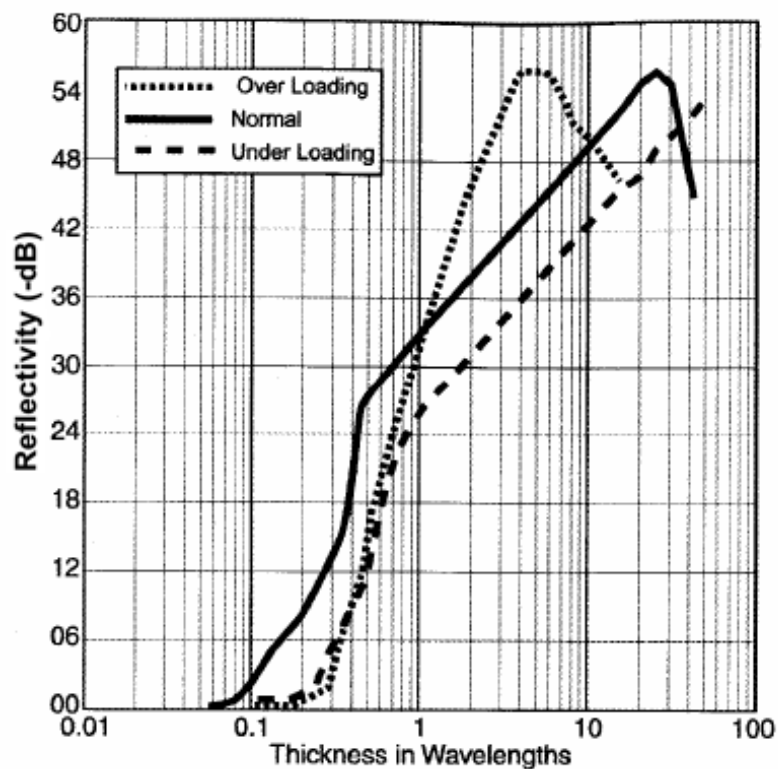


Figure 14. Variation in reflectivity with variation in thickness of carbon coating in an absorber [12]

In the Figure 14, reflectivity is same as the reflection loss or return loss as mentioned in the equation (20). In the figure, solid black line represents the favourable amount of carbon load in the foam. On increasing the quantity of carbon in the foam, the reflectivity

curve is shifted to left which means that a lot of carbon must be introduced onto the foam to achieve the same optimal amount of reflectivity characteristics.

Wavelength and frequency of the radio wave are inversely proportional to each other. Thus, the length of the pyramidal absorber can be from 10 cm to 25 cm depending upon the wavelength of the smallest possible frequency specified for the anechoic chamber. Pyramidal absorber of a length greater than or equal to 20 cm are mainly used for measuring the distance up to 10 m in an anechoic chamber where the requirement for NSA (National Security Agency) correlation of radiated RF immunity better than ± 4 dB must be fulfilled for the frequency ranging from 30 MHz to 1 GHz. According to IEC/EN 61000-4-3, the requirement for immunity test starting at 80 MHz can be fulfilled already with a pyramid of length 7.5 cm. Even pyramids of sizes 20 cm to 30 cm are sufficient for the measurement in the frequency range of greater than or equal to 1 GHz. [18]

Figure 15 is a technical drawing of square shaped broadband pyramidal absorber that is used in the anechoic chamber.

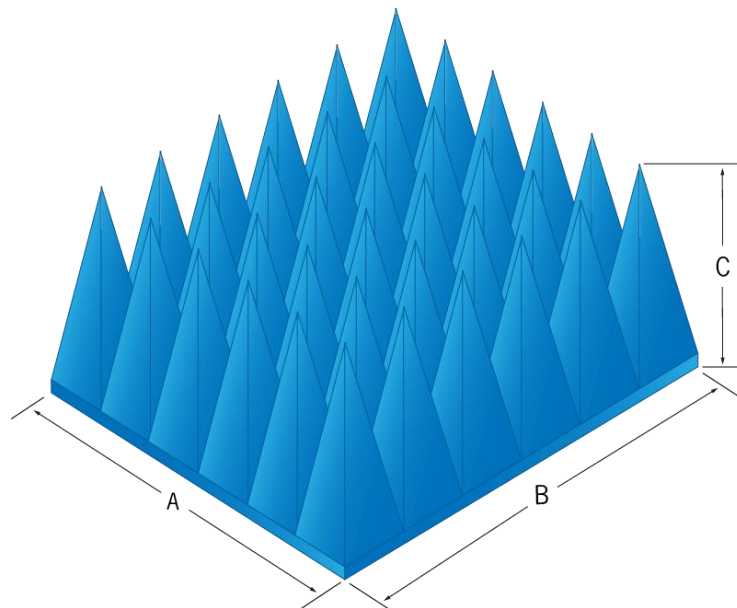


Figure 15. Technical drawing of square shaped pyramidal absorber [19]

The minimal height C (in Figure 15) of the pyramidal absorber can range from 2 or 3 inches for millimetre-wave absorbers to 12 feet for UHF (Ultra High Frequency) and VHF (Very High Frequency) absorbers. Almost all the square shaped pyramidal absorbers are manufactured with a 2×2 (A \times B) feet base which has become the standard size in all the industries. [20]

Typical reflectivity of the pyramidal absorber at normal incidence based on its thickness and the frequency specified can be seen in the Table 1. The reflectivity of the absorber is stated in the table as -dB.

Table 1. Typical performance of pyramidal absorber [12]

Table 3.1 Pyramidal Absorber Performance

Type	Height, cm (in.)	Weight, kg (lb)	Tips per piece	Normal Incidence Reflectivity, GHz									
				0.12	0.3	0.5	1.0	3.0	6.0	10.0	18.0	36	50
P-4	10.9(4.3)	1.4(3)	144					30	35	42	50	50	50
P-6	15.2(6)	1.6(3.5)	100					32	40	45	50	50	50
P-8	20.3(8)	2.0(4.5)	64				30	37	45	50	50	50	50
P-12	30.5(12)	2.7(6.0)	36				35	40	45	50	50	50	50
P-18	45.7(18)	5.4(12)	16			30	37	40	45	50	50	50	>45
P-24	61(24)	7.7(17)	9		30	35	40	45	50	50	50	50	>45
P-36	91.4(36)	10.9(24)	4		35	37	42	50	50	50	50	50	>45
P-48	121.9(48)	17(38)	2	28	35	40	50	50	50	50	50	50	>45
P-72	182.9(72)	23(50)	1	33	40	45	50	50	50	50	50	50	>45

Note: Base dimensions are 0.61 m²(2 ft²). Power rating is 0.08 W/cm²(0.5 W/in.²).

Similarly, the reflection coefficient of the pyramidal absorber as a function of incident angle can be seen in the Figure 16 below.

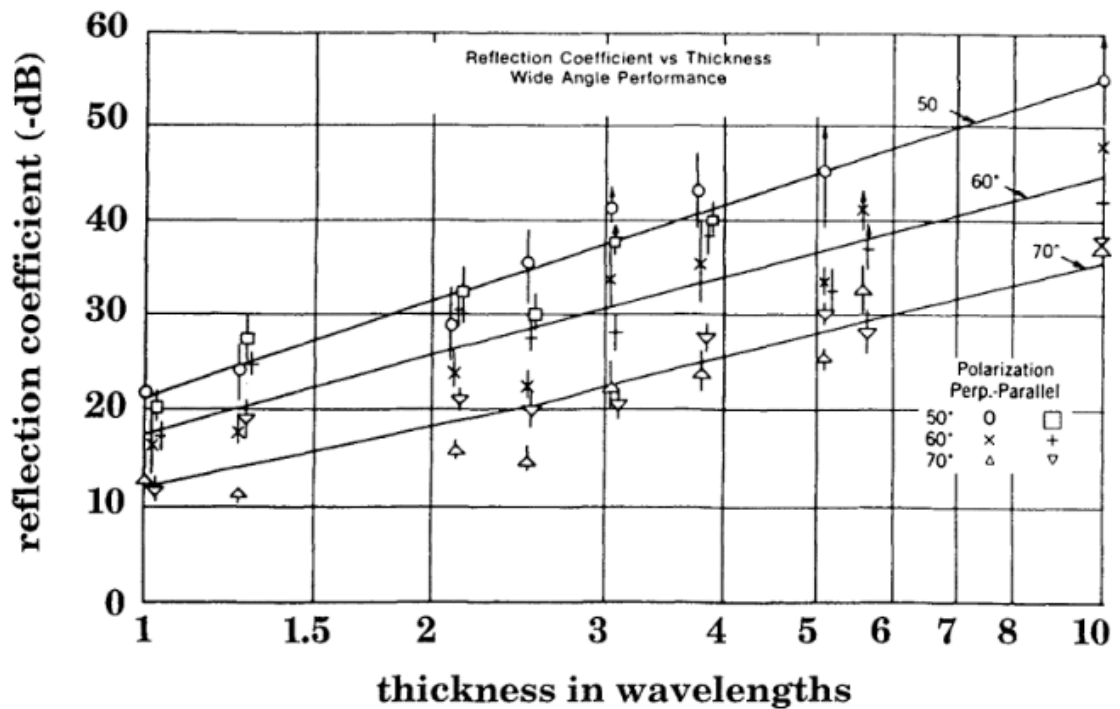


Figure 16. Carbon-filled pyramidal absorbers performance as a function of incident angle [21]

In the Figure 16, the reflection coefficient of the pyramidal absorbers is plotted against its thickness in wavelengths measured at 3 different angles (50, 60 and 70 degrees) of the incident wave. The plot suggests that the thickness of the absorber increases (compared to the wavelength) for the better performance of the anechoic chamber. Similarly, the plot also illustrates that the reflectivity is increased when angle of incident wave is increased and vice versa. This means that pyramidal absorbers give the best result when its tip are pointed towards the incident wave source. In some narrow anechoic chambers when the angle of incidence at the sidewalls reaches 70 degrees, Figure 16 suggests that the reflection coefficient for the 4λ pyramidal absorber can be as high as -25 dB. [20]

4.1.2 Ferrite Tile Absorbers

Ferrite tiles absorbers are magnetic absorbers [22]. They can be a suitable alternative to the traditional foam-type absorber for building new or upgrading the older anechoic chambers for radiated emission and immunity measurements. They are used in the anechoic chambers where maximum absorption (below 100 MHz) and compact size is required for attenuation of plane wave reflections. For example, a small box anechoic chamber can be made from the ferrite tiles for low frequency measurements. Ferrite tiles by nature are resistant to fire, chemicals and humidity. [23]

Ferrite tile absorbers are manufactured from solid ferrite which is a class of ceramic material with cubical crystalline structure and the molecular formula $MOFe_2O_3$; MO is combination of two or more divalent (two electrons in valence shell) metal oxides where Fe_2O_3 are iron oxides. These different types of metal oxides establish magnetic and absorptive properties in the ferrite. The metal oxides are generally soft metal oxides like zinc, copper, nickel or manganese oxides. [24]

Ferrite tile absorbers are available in two different forms, flat ferrite tiles and grid ferrite tiles. Flat ferrite tiles are about 6 mm in thickness, whereas the thickness is approximately 20 mm in a grid construction. Loss tangent and permeability are the two key elements that determines the behaviour of a ferrite tile absorber. Since loss tangent and permeability changes with frequency, it is quite difficult to design the frequency response of a ferrite tile over a wide frequency range. But with appropriate design, decent absorbing performance can be obtained over the frequency range between 30 MHz to 1000 MHz. [22;4]

The main principle that ferrite tiles work is that its impedance is matched to the impedance of free space. Besides, both permittivity and permeability of ferrite tiles are complex that make it lossy. This is achieved such that the ratio of permeability to the ratio of permittivity is approximately 377 ohms which is the impedance of the free space. The typical property of the ferrite tile is given by the equation (21).

$$\mu_r = \epsilon_r = 60(2 - j) \quad (21)$$

From Equation (21), the character impedance of the ferrite tile same as that of free space can be calculated as:

$$Z_0 = 377 \sqrt{\frac{\mu_r}{\epsilon_r}} = 377 \Omega \quad (22)$$

The reflection coefficient and the wave impedance of the ferrite tile can be calculated by using equations (18) and (19) respectively. Since the tile thickness is smaller than the wavelength at about 30 MHz frequency which is also the minimum frequency required by the FCC (Federal Communications Commission) and European standards, therefore [22]:

$$\tanh\left(j \frac{2\pi f d}{c} \cdot \sqrt{\mu_r \epsilon_r}\right) \rightarrow j \frac{2\pi f d}{c} (\sqrt{\mu_r \epsilon_r}) \quad (23)$$

Hence, equation (18) can be expressed as:

$$Z_{in} \approx j\mu_r \cdot \frac{2\pi f d}{c} \quad (24)$$

Thus, at low frequency wherever equation (23) is valid, the impedance of the ferrite tile (equation (24)) does not depend on the complex permittivity at low frequency [22]. Substituting equation (24) and $\mu_r = \mu_r' - j\mu_r''$, equation (19) can be written as:

$$\rho_l = \frac{\left(\frac{2\pi f d}{c} \mu_r'' - 1\right) + j \left(\frac{2\pi f d}{c} \mu_r'\right)}{\left(\frac{2\pi f d}{c} \mu_r'' + 1\right) + j \left(\frac{2\pi f d}{c} \mu_r'\right)} \quad (25)$$

The tile thickness at 30 MHz frequency is designed so that $\frac{2\pi fd}{c} \cdot \mu_r \rightarrow 1$, substituting equation (20) reflection loss (equation (20) can be written as:

$$RL = 20 \log_{10}(\rho_l) \approx -20 \cdot \log_{10} \left(\frac{2\mu_r''}{\mu_r'} \right) \approx -20 \log_{10}(2 \cdot \tan \delta_M) \quad (26)$$

Equation (26) shows the ferrite tile relation with reflectivity and tangential loss of the intrinsic permeability. Better performance can be achieved by increasing the tangential loss of the intrinsic permeability of the ferrite tile absorber. [22]

The responsive bandwidth of the ferrite tile can be also increased by placing ferrite tiles on the top of a dielectric spacer. Dielectric spacer is generally made up of wood and hence, the maximal responsiveness of the ferrite tile can be achieved by differing the thickness of the wood. Optimizing the thickness of both tile and dielectric spacer can shift the reflection loss performance from 600-1500 MHz. In case, if more bandwidth is required, engineered hybrid absorbers using specially designed and matched dielectric absorbers to the ferrite tiles like pyramidal and wedge-shaped absorber are needed. [23]

The ferrite tile with dielectric spacer attached to the metallic surface can be seen in the Figure 17 below.

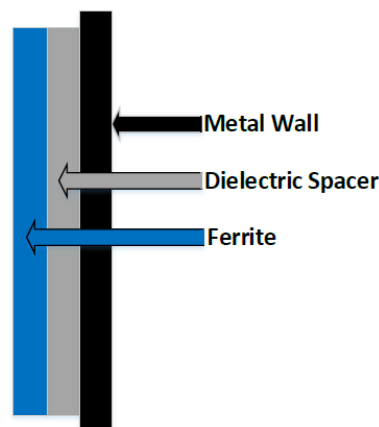


Figure 17. Ferrite tile mounted on metal surface [23]

Similarly, Figure 18 shows the variation of bandwidth with the increasing thickness of a dielectric spacer. The data shown in the figure can be used to calculate the effective (equation (27)) permeability of the tile if there are any air gaps present in between the tiles.

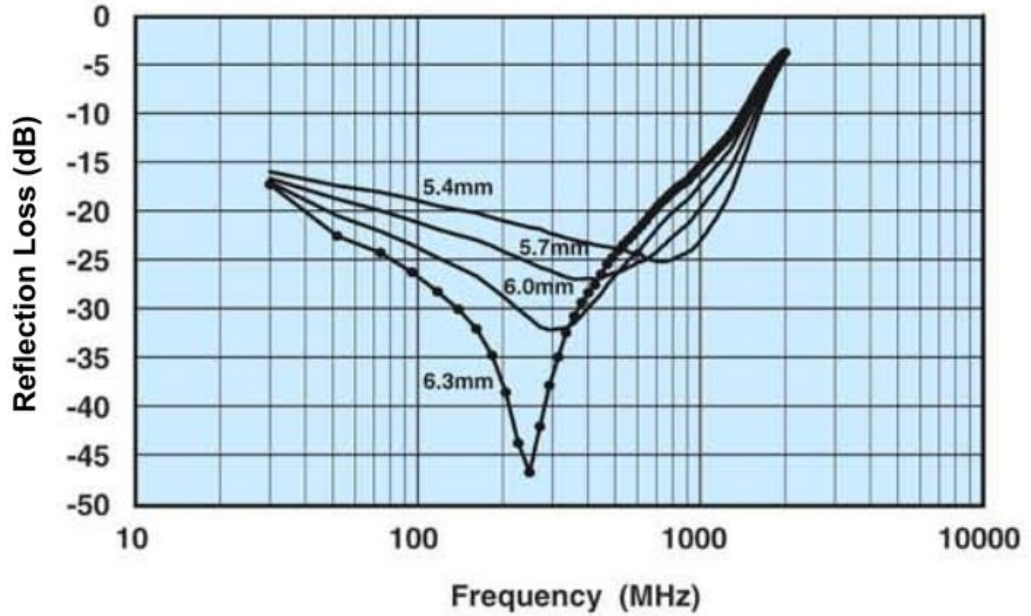


Figure 18. Variation of reflection loss with dielectric spacer thickness [23]

When placing the ferrite tile next to each other, it is very much essential to maintain minimal gap between each tile. Since ferrite tiles have permeability much bigger than 1, the air gaps present in between the tile can seriously affect the performance of an absorber. Therefore, many EMC and RF related companies are manufacturing the ferrite tiles in 20 mm² rather than manufacturing the tiles of normal dimension 100 mm² that helps to reduce the possible number of gaps remarkably. [12;22]

It has been found out that the impact of air gap between the tiles is analogous to the air gap that exists in between the iron core of the AC (Alternating Current) power transformer. Based on the formula of transformer core air gap, a theory has been introduced to determine the tiles effective permeability with air gaps as shown in equation (27). [22]

$$\mu_r^e = \frac{\mu_r}{1 + \frac{\Delta}{l}(\mu_r - \mu_{air})} \quad (27)$$

Where:

Δ = Air gap dimension that is perpendicular to the magnetic field line

l = Width of the ferrite tile

5 Anechoic chamber facility at Metropolia

The inside view of the anechoic chamber facility at Metropolia campus can be seen in the Figure 11. Similarly, the cross-sectional view of the chamber can be also seen in the Figure 19 below.

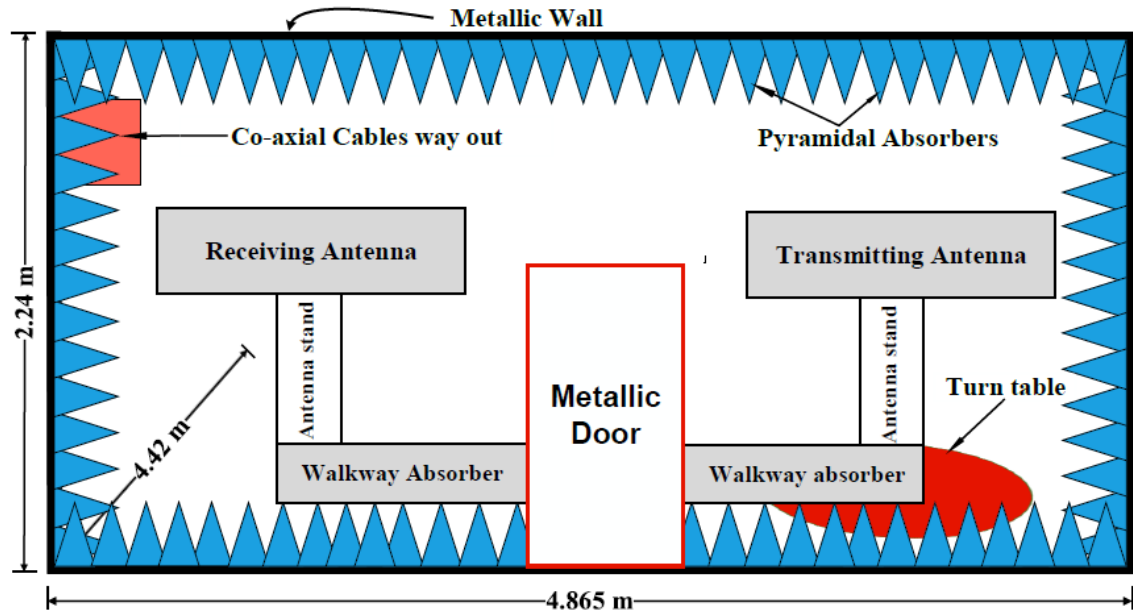


Figure 19. Model of the anechoic chamber facility the Metropolia

The chamber mainly uses pyramidal absorbers as a RF absorbing material. The pyramids are painted with latex blue to provide the chamber with good light reflectance [12]. The pyramids are on a square base like in the Figure 15 with 6x6 pyramids (36 pyramids in total). The dimension of each square shaped block with pyramids is 3600 cm². Figure 20 shows the geometry of a pyramid on a square base used in the chamber.

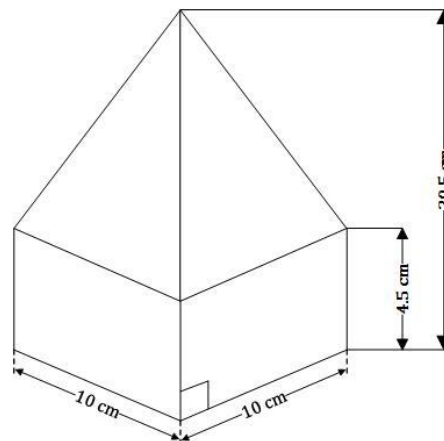


Figure 20. Pyramidal absorber dimensions

Looking at the dimension and the number of pyramids on the square base, the general characteristics of the pyramidal absorber used in the chamber can be determined from the Table 1 as represented in Table 2.

Table 2. General performance of the pyramidal absorber used in the chamber

Frequency (GHz)	0.5	1	3	6	10	18	30
Reflectivity (-dB)	30	35	40	45	50	50	50

There are also few black coloured rectangular box looking like structure inside the chamber called walkway absorbers which encapsulates the pyramidal absorbers. These absorbers are used inside the chamber so that antennas can be accessed whenever needed without damaging the pyramidal absorbers.

The transmitter antenna is attached to the Brüel & kjaer type 9640 turntable that can support up to 100 kg load [25]. The turntable can be controlled from the separate room by Brüel & kjaer turntable controller type 5997. With the help of the controller, the transmitter antenna can be rotated from 0-360 degrees and vice versa with the spacing of desired angle and acceleration. In addition, the turntable can be also controlled from the computer through LabVIEW software by using the NI (National Instruments) GPIB-USB-HS. The turntable and turntable controller used in the anechoic chamber and NI GPIB-USB-HS is shown in the Figure 21(a) and Figure 21(b) respectively.



Figure 21(a). Turntable and turntable controller [25], Figure 21(b). NI USB-GPIB-HS [26]

Though the chamber is fully anechoic, depending upon the performance of the pyramidal absorbers inside the chamber, resonance can occur at different modes. When the incident wave meets the reflected wave, the constructive and destructive interference pattern is formed that leads to resonance. The resonance results in the formation of standing waves in the space inside the chamber. The frequencies at which the resonance occurs

inside the chamber can be calculated from the measured dimensions of the anechoic chamber as shown in the equation (28) below.

$$f_{r(an)} = 150 \times \sqrt{\left(\frac{a}{l}\right)^2 + \left(\frac{b}{w}\right)^2 + \left(\frac{c}{h}\right)^2} \quad (28)$$

Where:

$f_{r(an)}$ = Resonance frequency of anechoic chamber [Hertz]

l = Length of the anechoic chamber = 4.865 metres

w = Width of the anechoic chamber = 4.42 metres

h = Height of the anechoic chamber = 2.24 metres

a, b and c = Positive integer constants

Some possible resonant modes of the space inside the Metropolia anechoic chamber can be seen in the Table 3 below. Only one of the constants can be zero at a time for a resonance to occur.

Table 3. Resonance frequencies of the anechoic chamber

<i>a</i>	<i>b</i>	<i>c</i>	<i>f_{r(an)} MHz</i>
1	0	1	73.72148392
1	1	0	45.85125899
1	1	1	81.15758444
1	1	2	141.559882
1	2	1	100.2079967
1	2	2	153.2784693
2	1	1	97.1518317
2	1	2	151.2981331
2	2	1	113.5498453
2	2	2	162.3151689
3	2	2	176.3502827
3	2	3	231.3449805
3	3	2	191.9841238
3	3	3	243.4727533

The maximum perpendicular distance from the transmitter antenna to the receiver antenna that can be considered for far field measurement inside the chamber is 2.5 metres. Therefore, the minimal frequency that can be used for far field measurement inside the anechoic chamber can be calculated using the well-known formula,

$$R \geq \frac{2D^2}{\lambda} \quad (29)$$

Where:

R = Far field distance

D = Diameter or length of an antenna

λ = Wavelength of the radio wave

Therefore, if an antenna is half wavelength long and far field starts at 2.5 metres distance from the transmitter antenna, equation (29) gives the minimum radio frequency that can be considered for testing a DUT (Device Under Test) inside the anechoic chamber as:

$$2.5 \geq \frac{c}{2f}$$

$$f \geq 60 \text{ MHz}$$

6 Reflectivity of the Anechoic Chamber

The reflectivity of the anechoic chamber was measured using two different types of method which are VSWR (Voltage Standing Wave Ratio) method and APC (Antenna Pattern Comparison) method. In the beginning, the main idea was to use only VSWR method. Later, it was decided to use APC method also so that results from both methods can be compared and hence, it can be investigated if calculated reflectivity values from both methods are similar. Consequently, this also helped to know if the calculated reflectivity value of the chamber was correct.

6.1 VSWR Method

When two identical waves oscillating either in the same direction or in the opposite direction meet each other either, there of the conditions are valid which are as follows:

- 1) They pass right through each other
- 2) They momentarily cancel out each other totally which is called destructive interference
- 3) They momentarily strengthen each other increasing the amplitude of the of the wave which is called constructive interference

When transmitter antenna is kept stationary and the receiver antenna is moved along the perpendicular, parallel and upward direction with respect to the axis of the chamber, VSWR method assumes that there exists a point P in the free space inside the anechoic chamber where the direct signal and the reflected signal meet each other and thus, interference pattern is formed. [27]

The oscillating reflected signal are superimposed with the direct signal and thus varies the amplitude of the direct signal at that point. Though the amplitude of the signal varies on changing the distance between the antennas and variations in the far-field conditions, the place where the two wave meets forms a ripple like that of standing wave. The maximum and minimum value of the ripple can be used to find the reflectivity of the anechoic chamber. [27]

6.1.1 Measurement Procedure

Figure 22 shows the measurement setup for the VSWR method. Two identical microstrip dipole antennas tuned at 735 MHz were used as a transmitter and a receiver antenna. Since the reflectivity measurement is based on the maximum and minimum value of the electric field, the antennas were vertically polarized. For a standing wave detector, Agilent 8741ET RF network analyzer was used which was placed outside of the anechoic chamber.

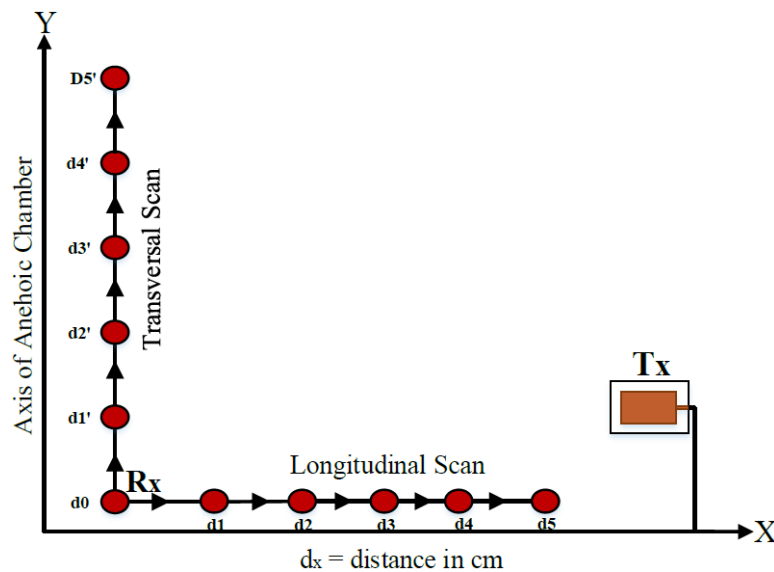


Figure 22. Measurement setup for VSWR method and APC method

At first, the receiver antenna Rx and transmitter antenna Tx were placed directly facing to each other at point d0 which was also taken as a reference point. The transmitter antenna was kept stationary but it can be rotated for pattern measurements with the help of turn table and the turntable controller.

For recording the standing wave curve, the receiver antenna was moved along the axis of the chamber (transversal line from the transmitter antenna) and towards the antenna. Besides, three conditions were considered for recording the VSWR curve which are described in short below:

- 1) The distance between the receiver antenna and the transmitter antenna was 225 centimetres from the reference point. The receiver antenna was moved from the reference point towards the transmitter antenna with the spacing of 2 centimetres. Total of the 30 standing wave magnitudes were recorded and the final distance between

the antennas was 80 centimetres when it was decided to record the final magnitude for the longitudinal scanning.

- 2) The receiver antenna was moved along the axis of the anechoic chamber with the spacing of 2 centimetres from the reference point until the distance from the reference point was 40 centimetres. Total of the 21 standing wave magnitudes were recorded for this measurement process.
- 3) The receiver antenna was moved along the axis of the chamber with the spacing of 10 centimetres from the reference point till the corner of the chamber which lies 121 centimetres away from the reference point. The measurements were taken at 13 different positions. At each position, the receiver antenna was turned towards 5 different directions (roughly 18 degrees at a time) until it was totally cross polarized with the transmitter antenna. The average magnitude was calculated from the recorded measurements for each position.

The reflectivity of the chamber R was then calculated from maxima (δ_1) and minima (δ_2) of the recorded interference pattern using the equations below.

$$R(dB) = 20 \cdot \log\left(\frac{E_r}{E_d}\right) = 20 \cdot \log\left(\frac{10^{\frac{\delta}{20}} - 1}{10^{\frac{\delta}{20}} + 1}\right) \quad (30)$$

Where:

$$\delta = \delta_1 - \delta_2$$

As per the CISPR 16-4-1 [28], the value of VSWR should not exceed 6 dB to pass the radiated emission test site that is,

$$VSWR[1] = \frac{E_{Max}[V/m]}{E_{Min}[V/m]} \leq 2 \quad (31)$$

$$VSWR[dB] = E_{Max}[dB\mu V] - E_{Min}[dB\mu V] \leq 6 \text{ dB} \quad (32)$$

Where:

E_{MAX} = Maximum electric field strength

E_{MIN} = Minimum electric field strength

6.1.2 Measurement Results and Calculations

The measurements taken at different conditions were plotted in the Excel and the VSWR curve obtained can be seen in the Figure 23, Figure 24 and Figure 25. The VSWR curve were then enveloped to get the maxima and minima of the interference pattern which can be seen in all the three figures. The pattern level 'a' was considered 0.00 dB as the aspect angle is 0 degree.

Since the amplitude varies at different points in the chamber, it is certain to get more than one values of reflectivity. So, two areas A and B were selected in each VSWR curve and two reflectivity values were calculated in each case. The maximum value calculated from all the curves was considered as the reflectivity of the anechoic chamber.

Calculation 1: When receiver antenna was moved towards the transmitter antenna

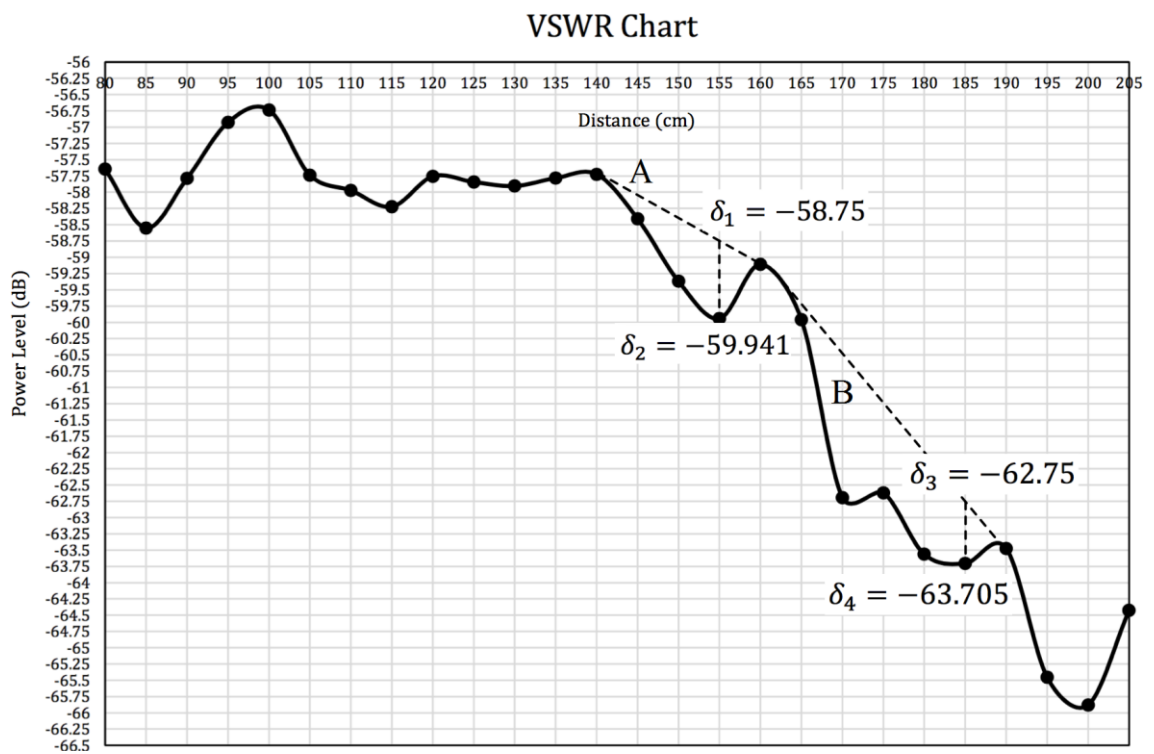


Figure 23. VSWR chart on receiver antenna towards the transmitter antenna

At area A:

$$\delta(A) = \delta_1 - \delta_2 = -58.75 - (-59.941) = 1.191 \text{ dB}$$

At area B:

$$\delta(B) = \delta_3 - \delta_4 = -62.75 - (-63.705) = 0.955 \text{ dB}$$

Thus, using equation (30), the reflectivity of the chamber was calculated at the area A and area B as,

$$R(A) = -23.292 \text{ dB}$$

$$R(B) = -25.205 \text{ dB}$$

Calculation 2: When receiver antenna was moved along the axis of the chamber

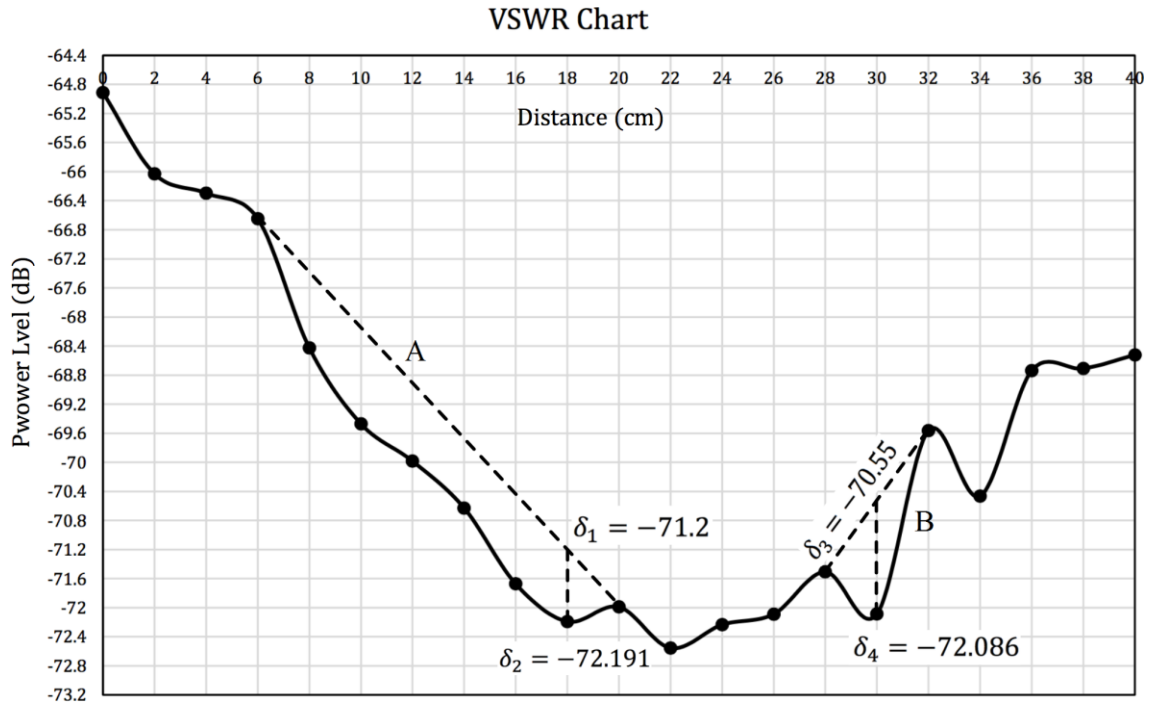


Figure 24. VSWR chart on moving receiver antenna along the axis of the chamber

At area A:

$$\delta(A) = \delta_1 - \delta_2 = -71.20 - (-72.191) = 0.991 \text{ dB}$$

At area B:

$$\delta(B) = \delta_3 - \delta_4 = -70.55 - (-72.086) = 1.536 \text{ dB}$$

Thus, using equation (30), the reflectivity of the chamber was calculated at the area A and area B as,

$$R(A) = -24.884 \text{ dB}$$

$$R(B) = -21.091 \text{ dB}$$

Calculation 3: When receiver antenna was moved along the axis of the chamber turning at five different angles at each position

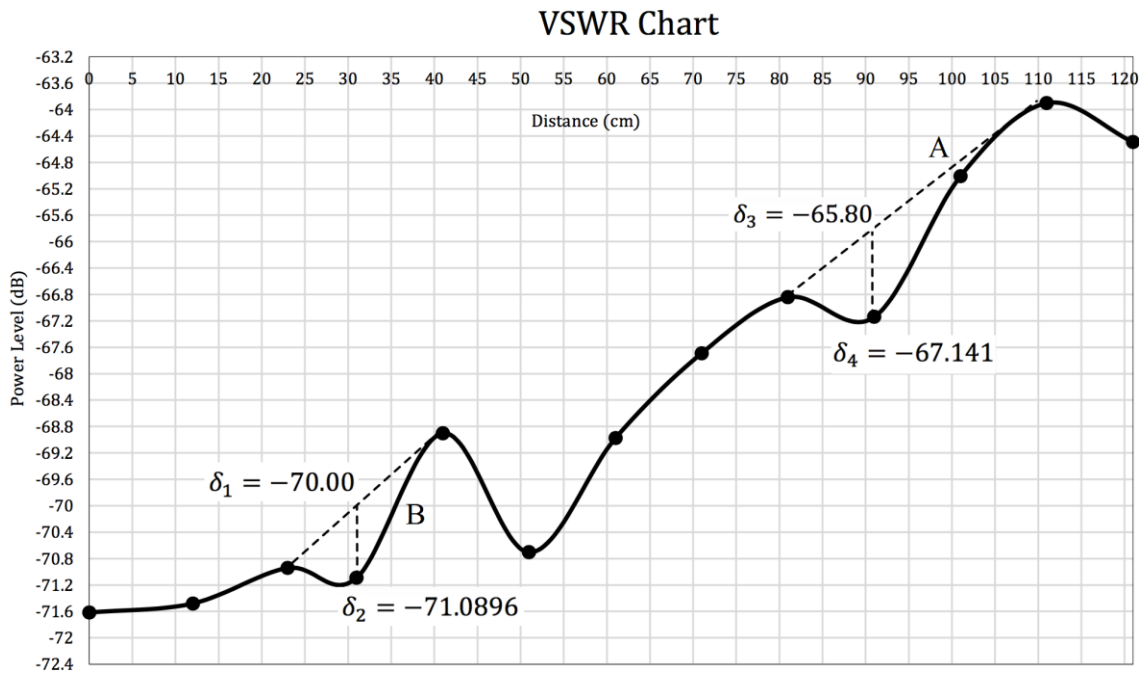


Figure 25. Average VSWR chart on moving receiver antenna at different angles along the chamber axis

At area A:

$$\delta(A) = \delta_1 - \delta_2 = -70 - (-71.0896) = 1.0896 \text{ dB}$$

At area B:

$$\delta(B) = \delta_3 - \delta_4 = -65.80 - (-67.141) = 1.341 \text{ dB}$$

Thus, using equation (30), the reflectivity of the chamber was calculated at the area A and area B as,

$$R(A) = -24.062 \text{ dB}$$

$$R(B) = -22.265 \text{ dB}$$

The 6 reflectivity values calculated in all three cases were quite near. Comparing to all the reflectivity values, the maximum reflectivity value was obtained at area B (Figure 23) when receiver antenna was moved towards the transmitter antenna. Hence, the reflectivity of the chamber was determined as:

$$\text{Reflectivity of the anechoic Chamber } (R) = -21.091 \text{ dB}$$

6.2 APC Method

When the radiation pattern of an antenna is recorded at discrete positions along the axis of the chamber (transversal line), there occurs a small variation in the recorded patterns. These variations can be seen when all the recorded patterns are superimposed on the top of each other. Hence, the magnitude of these variations can be used to determine the reflectivity of the anechoic chamber. [27]

6.2.1 Measurement Procedure

The measurement setup for the APC method was same as in the VSWR method. The difference was that the receiver antenna was moved only along the axis of the chamber. The antennas were vertically polarized and the radiation patterns of the transmitter antenna were recorded at five different positions from the reference point with the spacing of 10 centimetres. The reflectivity was then calculated using the equation (30) substituting the value of maximum and minimum field detected from the variation obtained after superimposing all the patterns together.

6.2.2 Measurement Results and Calculations

The measured radiation patterns at five different positions on the axis of the chamber plotted in the rectangular coordinate system can be seen in the Figure 26 below.

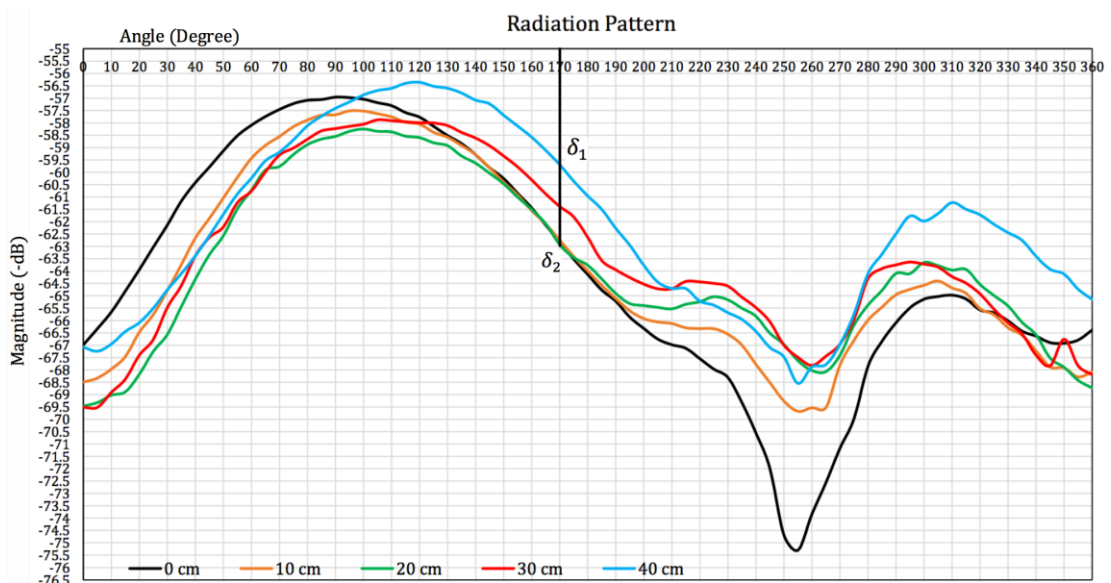


Figure 26. Radiation pattern rerecorded at discrete positions on the axis of the chamber

In the Figure 26, solid black line represents the radiation pattern recorded at reference position (0 cm) i.e. when the antennas were directly facing at each other. Similarly, δ_1 and δ_2 were the maximum and minimum field detected after superimposing the patterns.

In the Figure 26, it can be seen that there is difference of about -2 dB in magnitude from the reference radiation pattern to the pattern recorded at 10 centimetres at an angle between 0-60 degrees. After, the pattern seems to be quite coinciding with the main lobe of the reference pattern. Similarly, the radiation patterns taken at distance of 10, 20 and 30 centimetres from the reference position are coinciding with each other with little difference only.

The pattern taken at distance of 40 centimetres from the reference position is coinciding with the patterns taken at 10, 20 and 30 centimetres only till 100 degrees. The main lobe of the pattern is deviating outward from 100 degree by -2 dB to -3 dB even from the reference pattern. The pattern recorded at 30 centimetres is also deviating outward of the reference pattern from an angle of 125 degree.

Similarly, the radiation patterns plotted in polar coordinates can be seen in in the Figure 27 below. In the figure, it can be clearly seen that how radiation pattern is varying on moving the receiver antenna along the axis of the anechoic chamber.

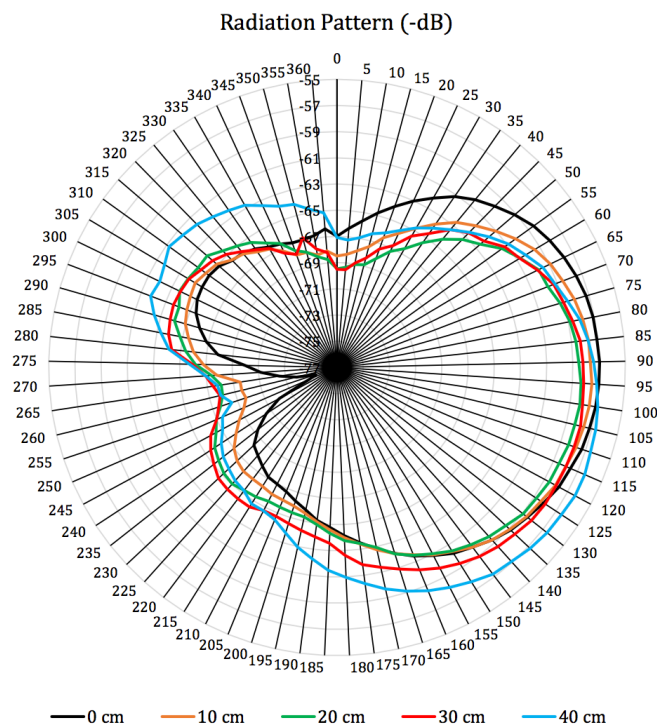


Figure 27. Polar plot of Radiation Patterns

Since in APC method, the reflectivity values differ with angles, 6 different angles were selected to calculate the reflectivity of the chamber. Hence, using the equation (30), the reflectivity levels of the anechoic chamber with the corresponding angles were calculated as:

Table 4. Reflectivity levels at corresponding angle

Angle (degree)	20	50	70	100	150	170
Reflectivity (-dB)	12.423	14.181	17.586	23.198	16.005	14.685

From the Table 4 above, the average reflectivity of the chamber was calculated as - 13.846 dB. However, the maximum value was selected to represent the reflectivity of the anechoic chamber. For an angle θ , the highest value of reflectivity can be represented in the interval $0 \leq \theta \leq 180$. Similarly, the superimposed radiation patterns (Figure 26 and Figure 27) also suggest that maximum reflectivity lies in between these angles.

7 Conclusion

The evaluation of the anechoic chamber was achieved by applying the most commonly used techniques known as VSWR method and APC method. Since the chamber was evaluated at only one frequency (735 MHz), it can be said at least that the anechoic chamber proved to be in quite smooth condition for the tests below 1 GHz.

Comparing the value of VSWR to the standard mentioned in the CISPR 16-4-1, the obtained result meet the requirement to pass the radiated emission test site. The maximum value of VSWR obtained during the entire measurement process was 1.536 dB which is much less than the required VSWR value as mentioned in the standard CISPR 16-4-1. Similarly, anechoic chamber of reflectivity at least -20 dB is recommended for the tests below 1 GHz. The obtained reflectivity value of the chamber using VSWR method was 1 dB less than the minimum value recommended for the reflectivity. In addition, looking at the performance of the pyramidal absorber below 1 GHz (Table 2), it can be said that the value obtained from the VSWR method is quite satisfactory.

Though the results obtained from the APC method varies from the VSWR method, Appel-Hansen [27,495] suggests that same kind of results can be obtained using VSWR method on moving the receiving antenna towards the transmitting antenna with different aspect angles. However, the reflectivity value did not exceed 6 dB which means the test site passed the radiated emission requirement as mentioned in CISPR 16-4-1. Besides, larger number of patterns should be taken to get the accurate results in APC method which requires considerable amount of time and analysis work. On the contrary, the specifications of anechoic chamber nowadays generally include the maximum value of reflectivity calculated using VSWR method as it helps to know the maximum inconsistency in the measured results.

For the better characterization of the chamber, the values of reflectivity can be calculated at various frequencies. Similarly, the attenuation of the chamber can be investigated to study its shielding effectiveness. The resonance frequencies of the chamber can be identified and thus improvement can be done in those areas if measurements must be done in those frequency ranges. Better performance of the anechoic chamber complying with the industrial standards can be achieved by replacing the damaged pyramid blocks as there are lot of pyramids with broken tips and with proper arrangement of absorbers around the testing region.

References

- [1] L. V. Blake and M. W. Long, *Antennas Fundamentals, Design, Measurement*, 3rd ed., D. R. Kay, Ed., Raleigh, NC: SciTech Publishing, 2009.
- [2] National Radio Astronomy Observatory, "Inverse-Square Law of Propagation," [Online].
Available: http://www.gb.nrao.edu/GBTopsdocs/primer/inverse-square_law_of_propa.htm.
[Accessed 6 April 2017].
- [3] B. k. Chung, "Anechoic Chamber Design," Springer Singapore, Singapore, 2015.
- [4] C. A. Balanis, *Antenna Theory-Analysis and Design*, 4th ed., NJ: John Wiley & Sons, Inc, 2016.
- [5] J. W. Healy, "The American Radio Relay League (ARRL)," June 1991. [Online].
Available: <https://www.arrl.org/files/file/Technology/tis/info/pdf/9106023.pdf>.
[Accessed 22 March 2017].
- [6] Radio-Electronics.com, "Dipole Antenna/Aerial Tutorial," [Online].
Available: <http://www.radio-electronics.com/info/antennas/dipole/dipole.php>.
[Accessed 22 March 2017].
- [7] Radio-Electronics.com, "Dipole Antenna Length Calculation & Formula," 23 March 2017. [Online].
Available: <http://www.radio-electronics.com/info/antennas/dipole/length-calculation-formula.php>.
- [8] S. Mess-Elektronik, "SCHWARZBECK Mess-Elektronik," n.d.. [Online].
Available: <http://schwarzbeck.de/Datenblatt/biconall.pdf>.
[Accessed 5 March 2017].
- [9] J. K. f. Hafner, "A Study of The Properties of Biconical Antenna," New Jersey Institute of Technology, Newark, NJ, 1968.
- [10] K. W.H. and G. E.S., "Antenna measurements," *Proceedings of the IEEE*, vol. 66, no. 4, pp. 483-507, April 1978.
- [11] IEEE Digital Library, "149-1979 - IEEE Standard Test Procedures for Antennas," IEEE, 1979.
- [12] L. H. Hemming, "Electromagnetic Absorbing Materials," in *Electromagnetic Anechoic Chambers:A Fundamental Design and Specification Guide*, 1st ed., NJ, USA, Wiley-IEEE Press, 2002, pp. 27-48.

- [13] A. Woods, "USQ ePrints," n.d. June 2006. [Online].
Available:https://eprints.usq.edu.au/2367/1/WOODS_Andrew-2006.pdf.
[Accessed 2 February 2017].
- [14] G. Dash, "How RF Anechoic Chambers Work," Ampyx LLC, 1999.
- [15] Machinerieen Naamlooze Vennootschap. French Patent 802 728, 1936.
- [16] I. Emerson & Cuming Microwave Products, "LAIRD," n.d.. [Online].
Available:<http://www.eccosorb.com/683be594-bcb2-404c-a440-0804f968a82f/resource-white-papers-display.htm>.
[Accessed 26 February 2017].
- [17] E. Technologies, "Microwave Absorber," Euro Technologies, n.d.. [Online].
Available:<http://www.euro-technologies.eu/en/products/microwave-absorber/>.
[Accessed 27 February 2017].
- [18] B. F. Lawrance, *Anechoic Chamber, Past and Present*, Conformity Magazine, 2005.
- [19] Holland Shielding Systems BV, "Holland Shielding Systems BV," Holland Shielding Systems BV, [Online].
Available:<http://hollandshielding.com/320-Broadband%20hybrid%20pyramidal%20absorbers>.
[Accessed 7 March 2017].
- [20] B. F. Knott, *Radar Cross Section Measurements*, Raleigh: SciTech Publishing, Inc, 1993.
- [21] W. H. Emerson, "Electromagnetic Wave Absorbers and Anechoic Chambers through the Years," *IEEE Transactions on Antennas and Propagation*, Vols. AP-21, pp. 484-490, July 1973.
- [22] K. Liu, "Analysis of the Effect of Ferrite Tile Gap on EMC Chamber Having Ferrite Absorber Walls," in *IEEE*, Santa Clara, CA, USA, 1996.
- [23] Fair-Rite Products Corp, "Technical Information," [Online].
Available:http://www.elnamagnetics.com/wp-content/uploads/library/Fair-Rite-Documents/Ferrite_Tile_Absorbers_for_EMCTest_Chamber_Applications.pdf.
[Accessed 17 March 2017].
- [24] D. electronics, "EMI Filters and RF Shielding Products," 13 4 2014. [Online].
Available: <http://www.djmelectronics.com/rf-absorber.html>.
[Accessed 15 March 2017].

- [25] Brüel & Kjær Sound and Vibration, "Product Data," [Online].
Available: <https://www.bksv.com/media/doc/bp1617.pdf>.
[Accessed 16 April 2017].
- [26] National Instruments, "National Instruments," [Online].
Available: <http://www.ni.com/en-gb/support/model.gpib-usb-hs.html>.
[Accessed 16 April 2017].
- [27] J. Appel-Hansen, "Reflectivity Level of Radio Anechoic Chambers," *IEEE Transactions on Antennas and Propagation*, vol. 21, no. 4, pp. 490-498, 1973.
- [28] International Electrotechnical Commission, *CISPR 16-1-4*, International Electrotechnical Commission, 2008.

Longitudinal Scan Data

Distance (cm)	Magnitude (dB)
80	-57.645
85	-58.55
90	-57.788
95	-56.928
100	-56.735
105	-57.737
110	-57.974
115	-58.222
120	-57.757
125	-57.844
130	-57.905
135	-57.784
140	-57.724
145	-58.407
150	-59.369
155	-59.941
160	-59.108
165	-59.959
170	-62.691
175	-62.619
180	-63.562
185	-63.705
190	-63.474
195	-65.453
200	-65.881
205	-64.426
210	-63.588
215	-62.861
220	-64.16
225	-65.49

Transversal Scan Data

Distance (cm)	Magnitude (dB)
0	-64.911
2	-66.031
4	-66.297
6	-66.648
8	-68.424
10	-69.47
12	-69.984
14	-70.629
16	-71.672
18	-72.191
20	-71.99
22	-72.555
24	-72.235
26	-72.088
28	-71.507
30	-72.086
32	-69.564
34	-70.464
36	-68.739
38	-68.71
40	-68.522

Transversal Scan Data at different angles of antenna

Distance (cm)	Magnitude (dB)	Distance (cm)	Magnitude (dB)	Distance (cm)	Magnitude (dB)
0	-64.143	51	-65.717	101	-67.74
	-68.384		-69.102		-64.636
	-76.418		-72.244		-62.825
	-78.286		-74.885		-61.885
	-70.855		-71.58		-67.365
12	-66.932	71	-68.421	111	-63.491
	-69.962		-69.461		-61.776
	-70.906		-66.357		-60.416
	-75.379		-65.614		-66.467
	-74.219		-68.593		-67.954
23	-68.415	81	-68.632	121	-67.631
	-71.537		-67.694		-64.355
	-71.374		-64.309		-62
	-71.421		-64.253		-61.281
	-71.967		-69.324		-67.192
31	-67.465	91	-67.79		
	-70.59		-67.689		
	-71.466		-65.587		
	-71.217		-62.324		
	-74.71		-72.315		
41	-65.645	61	-66.082		
	-67.919		-68.889		
	-68.473		-70.006		
	-69.334		-69.277		
	-73.14		-70.623		

Distance (cm)	Average Magnitude (dB)
0	-71.6172
121	-64.4906
111	-63.903
101	-64.868
91	-67.0848
81	-66.8424
71	-67.6892
61	-68.9754
51	-70.7056
41	-68.9022
31	-71.0896
23	-70.9428
12	-71.4796